Author/s:
Hung, LW;Villemagne, VL;Cheng, L;Sherratt, NA;Ayton, S;White, AR;Crouch, PJ;Lim, SC;Leong, SL;Wilkins, S;George, J;Roberts, BR;Pham, CLL;Liu, X;Chiu, FCK;Shackleford, DM;Powell, AK;Masters, CL;Bush, AI;O'Keefe, G;Culvenor, JG;Cappai, R;Cherny, RA;Donnelly, PS;Hill, AF;Finkelstein, DI;Barnham, KJ

Title:
The hypoxia imaging agent Cu ii(atsm) is neuroprotective and improves motor and cognitive functions in multiple animal models of Parkinson's disease

Date:
2012-04-09

Citation:
Hung, L. W., Villemagne, V. L., Cheng, L., Sherratt, N. A., Ayton, S., White, A. R., Crouch, P. J., Lim, S. C., Leong, S. L., Wilkins, S., George, J., Roberts, B. R., Pham, C. L. L., Liu, X., Chiu, F. C. K., Shackleford, D. M., Powell, A. K., Masters, C. L., Bush, A. I. ,... Barnham, K. J. (2012). The hypoxia imaging agent Cu ii(atsm) is neuroprotective and improves motor and cognitive functions in multiple animal models of Parkinson's disease. Journal of Experimental Medicine, 209 (4), pp.837-854. https://doi.org/10.1084/jem.20112285.

Persistent Link:
https://hdl.handle.net/11343/234299

The hypoxia imaging agent Cu^{II}(atsm) is neuroprotective and improves motor and cognitive functions in multiple animal models of Parkinson's disease

Lin W. Hung,[1,6] Victor L. Villemagne,[1,7] Lesley Cheng,[5,6] Nicki A. Sherratt,[2,6] Scott Ayton,[1] Anthony R. White,[1,3] Peter J. Crouch,[1,3] SinChun Lim,[4,6] Su Ling Leong,[3,6] Simon Wilkins,[1] Jessica George,[1] Blaine R. Roberts,[1] Chi L.L. Pham,[3,6] Xiang Liu,[1,6] Francis C.K. Chiu,[8] David M. Shackleford,[8] Andrew K. Powell,[8] Colin L. Masters,[1] Ashley I. Bush,[1] Graeme O'Keefe,[8] Janetta G. Culvenor,[1,3] Roberto Cappai,[3,6] Robert A. Cherny,[1] Paul S. Donnelly,[4,6] Andrew F. Hill,[1,5,6] David I. Finkelstein,[1] and Kevin J. Barnham[1,2,6]

[1]The Mental Health Research Institute, [2]Department of Pharmacology, [3]Department of Pathology, [4]The School of Chemistry, [5]Department of Biochemistry and Molecular Biology, [6]Bio21 Molecular Science and Biotechnology Institute, the University of Melbourne, Victoria 3010 Australia
[7]Centre for PET, Austin Hospital, Heidelberg, Victoria 3084, Australia
[8]Centre for Drug Candidate Optimisation, Monash Institute of Pharmaceutical Sciences, Monash University, Parkville, Victoria 3052, Australia

Parkinson's disease (PD) is a progressive, chronic disease characterized by dyskinesia, rigidity, instability, and tremors. The disease is defined by the presence of Lewy bodies, which primarily consist of aggregated α-synuclein protein, and is accompanied by the loss of monoaminergic neurons. Current therapeutic strategies only give symptomatic relief of motor impairment and do not address the underlying neurodegeneration. Hence, we have identified Cu^{II}(atsm) as a potential therapeutic for PD. Drug administration to four different animal models of PD resulted in improved motor and cognition function, rescued nigral cell loss, and improved dopamine metabolism. In vitro, this compound is able to inhibit the effects of peroxynitrite-driven toxicity, including the formation of nitrated α-synuclein oligomers. Our results show that Cu^{II}(atsm) is effective in reversing parkinsonian defects in animal models and has the potential to be a successful treatment of PD.

Parkinson's disease (PD) is a common motor neurodegenerative disorder, with an average age of onset of 55 yr and disease duration of ∼20 yr (Dauer and Przedborski, 2003). It is a progressive and chronic disease characterized by dyskinesia, rigidity, instability, and tremors (Parkinson, 2002). The pathognomonic indicator of disease is the presence of Lewy bodies, which primarily consist of aggregated α-synuclein protein (Lewy, 1912). This is accompanied by the loss of monoaminergic neurons, of which dopamine-producing neurons within the substantia nigra pars compacta (SNpc) are the most prominent (Hassler, 1938).

Ideally, a therapy for PD would address these pathological features. However, current therapeutic strategies only give symptomatic relief of the motor impairment (Obeso et al., 2010). This is achieved by supplying a dopamine precursor (L-DOPA), by supplying dopamine agonists (e.g., pramipexole, bromocriptine), or by inhibiting dopamine breakdown (e.g., selegiline, a monoamine oxidase B inhibitor; Stowe et al., 2008). Alternately, surgical ablations or deep brain stimulation are used to empirically improve motor function (Trost et al., 2006). These treatments can

CORRESPONDENCE
Kevin J. Barnham:
kbarnham@unimelb.edu.au

Abbreviations used: 3-NT, nitrotryosine; 6-OHDA, 6-hydroxydopamine; ALS, amyotrophic lateral sclerosis; Cu^{II}(atsm), copper(II)diacetyl*bis*(*N*(4)-methylthiosemicarbazonato); LC-MS, liquid chromatography-mass spectrometry; MPTP, 1-methyl-4-phenyl-1,2,3,6-tetrahydropyridine; NMR, nuclear magnetic resonance; NO, nitric oxide; NOR, novel object recognition; NOS, NO synathase; ONOO−, peroxynitrite; PET, positron emission tomography; qPCR, quantitative real-time PCR; SIN-1, N-morpholinosydnonimine; SNpc, substantia nigra pars compacta; SOD, superoxide dismutase; tg, transgenic; TH, tyrosine hydroxylase; VMAT2, vesicular monoamine transporter 2.

D.I. Finkelstein and K.J. Barnham contributed equally to this paper.
C.L.L. Pham's present address is Dept. of Biology and Biochemistry, University of Bath, Claverton Down, Bath BA2 7AY, UK.

The Rockefeller University Press $30.00
J. Exp. Med. Vol. 209 No. 4 837-854
www.jem.org/cgi/doi/10.1084/jem.20112285

The Journal of Experimental Medicine

largely keep the symptoms of disease under control for years, but do not address the underlying neurodegeneration, and, as such, there is an urgent need to identify new disease-modifying strategies.

The underlying cause of PD is still debated, with numerous hypotheses suggested, including mitochondrial dysfunction, dopamine toxicity, oxidative stress, and misfolding and oligomerization of α-synuclein (Schulz, 2008). Although mutation of α-synuclein is associated with rare hereditary forms of the disease, PD is linked to ∼14 different genes that account for ∼5–10% of all PD cases (Thomas and Beal, 2007). This has contributed to the ambiguity of disease progression, and has hindered development of effective treatments that can target all aspects of disease.

One common factor in these pathways is the contribution of nitrosative stress. Nitrosative stress is caused by reactive nitrogen radicals, particularly peroxynitrite ($ONOO^-$), which is formed from a nonenzymatic and pH-dependent reaction of nitric oxide (NO) and superoxide (O_2^-), and is able to modify a wide range of cellular elements, including tyrosine nitration, cysteine (thiol) nitrosation, DNA oxidation, and lipid peroxidation (Beckman et al., 1990; Szabó et al., 2007; Reynolds et al., 2007). $ONOO^-$ has been implicated in the pathophysiology of several diseases (Szabó et al., 2007), including PD and amyotrophic lateral sclerosis (ALS; Beckman et al., 1993). Biochemically, $ONOO^-$ induces the nitration and aggregation of α-synuclein (Souza et al., 2000); these adducts are highly enriched in Lewy bodies of PD subjects (Giasson et al., 2000). Yu et al. (2010) recently demonstrated that nitrated α-synuclein is neurotoxic, with injection of nitrated α-synuclein into the SNpc of rats recapitulating many of the pathological features of PD.

The NO required for the formation of $ONOO^-$ is generated by NO synthase (NOS), in the brain. There are three isoforms of NOS: neuronal NOS (nNOS, type I), inducible NOS (iNOS, type II), and endothelial NOS (eNOS; type II; Ebadi and Sharma, 2003). These enzymes catalyze the formation of NO and citrulline from L-arginine. nNOS has been detected in the cerebellum, the hypothalamus, the striatum, and the medulla oblongata. iNOS is located predominately in microglia and astrocytes. eNOS has been detected in microvessels and motor neurons from rodents and humans. iNOS and nNOS have been implicated in PD-like pathology, as mutant mice lacking either iNOS or nNOS are protected against 1-methyl-4-phenyl-1,2,3,6-tetrahydropyridine (MPTP) toxicity (Przedborski et al., 1996; Dehmer et al., 2000). Similarly, 7-nitroindazole, a specific inhibitor of nNOS, also protects against MPTP (Schulz et al., 1995; Hantraye et al., 1996b). The potential role of NO in PD pathogenesis has been extensively reviewed (Giasson et al., 2000; Oehlberg et al., 2008; Pierucci et al., 2011). Importantly, nitrosative stress is not only a part of the pathological process in PD animal models (Ferrante et al., 1999; Watabe and Nakaki, 2008; Gupta et al., 2010) but also in human patients with increased nitrotyrosine (3-NT) levels observed in both the blood and brain (Good et al., 1998; Duda et al., 2000; Giasson et al., 2000).

The body's endogenous natural scavenger of $ONOO^-$ is uric acid, and lowered levels of uric acid have been associated with a higher risk of PD (Hooper et al., 1998). Conversely, patients suffering from gout, a result of increased uric acid levels, are protected against PD (Alonso et al., 2007; De Vera et al., 2008). Serum levels of uric acid and its metabolites are currently being assessed as potential biomarkers for PD (Hooper et al., 1998; de Lau et al., 2005; Cipriani et al., 2010). These results suggest that agents that can inhibit the actions of $ONOO^-$ may have therapeutic potential in PD.

Radiolabeled copper(II)diacetyl*bis*(*N*(4)-methylthiosemicarbazonato), (Cu^{II}[atsm]) is currently under clinical investigation as a positron emission tomography (PET) imaging agent for myocardial ischemia and hypoxic imaging in malignant tumors (Lewis et al., 2001). We have identified that this compound is also able to function as a highly effective scavenger of $ONOO^-$, inhibiting its toxicity, as well as the nitration and oligomerization of α-synuclein in vitro. As Cu^{II}(atsm) is capable of crossing the blood–brain barrier (Fodero-Tavoletti et al., 2010), the compound was assessed for its ability to rescue PD-relevant phenotypes in multiple animal models.

RESULTS

Cu^{II}(atsm) inhibited $ONOO^-$–induced aggregation of α-synuclein

To investigate whether Cu^{II}(atsm) was able to directly alter $ONOO^-$ activity (absorbance at 203 nm), the time-dependent degradation of $ONOO^-$ was monitored by UV-visible spectroscopy. $ONOO^-$ in a high pH solution has a half-life of 53 ± 3 min (Fig. 1 a). However, in the presence of Cu^{II}(atsm), the rate of $ONOO^-$ degradation was increased in a dose-dependent manner. Incubation with Cu^{II}(atsm) at 10 µM resulted in an $ONOO^-$ half-life of ∼11.6 ± 0.5 min (Fig. 1 a).

To establish whether Cu^{II}(atsm) is able to inhibit $ONOO^-$-mediated nitration of proteins, its ability to prevent the nitration and oligomerization of α-synuclein was assessed. As shown in previous studies, the reaction of $ONOO^-$ and α-synuclein leads to the nitration of tyrosine residues and the formation of oligomers (Fig. 1 b; Souza et al., 2000; Paxinou et al., 2001). Cu^{II}(atsm) inhibited this reaction in a dose-dependent manner (Fig. 1 c). Using an ELISA method (Fig. 1 d), Cu^{II}(atsm) had an IC_{50} of 1 µM compared with 63 µM for uric acid, which is an endogenous scavenger of $ONOO^-$.

Given the significant role that α-synuclein aggregation plays in PD, we ascertained whether Cu^{II}(atsm) was specific for inhibiting $ONOO^-$-induced α-synuclein aggregation, or if Cu^{II}(atsm) could inhibit other modes of α-synuclein aggregation. First we ascertained using nuclear magnetic resonance (NMR) spectroscopy that there was no direct interaction between α-synuclein and Cu^{II}(atsm) as two-dimensional [^{1}H,^{15}N] HSQC spectra of uniformly ^{15}N-labeled α-synuclein were unaffected by titrating in increasing concentrations of Cu^{II}(atsm). α-Synuclein self-aggregates over time to form amyloid fibrils that can be monitored by Thioflavin T fluorescence and electron microscopy. Incubation with Cu^{II}(atsm)

did not inhibit the formation of α-synuclein fibrils (unpublished data). α-Synuclein reacts with dopamine to generate soluble oligomers, the formation of which is facilitated by oxidation of methionine sulfur atoms to sulfoxide (Cappai et al., 2005; Leong et al., 2009). Cu^{II}(atsm) did not inhibit dopamine induced formation of soluble oligomers of α-synuclein (unpublished data), nor does Cu^{II}(atsm) have any measurable superoxide dismutase (SOD)–mimetic activity (unpublished data), indicating that Cu^{II}(atsm) is not a broad spectrum antioxidant.

Cu^{II}(atsm) inhibited N-morpholinosydnonimine (SIN-1)–mediated toxicity and nitrosative stress in differentiated SH-SY5Y cells

The ability of Cu^{II}(atsm) to inhibit $ONOO^-$ toxicity on differentiated human neuroblastoma SH-SY5Y cells was investigated. The differentiated neurons have increased levels of synaptophysin and TH upon differentiation (unpublished data), which is consistent with them being a better model for dopaminergic neurons. The differentiated cells were treated with

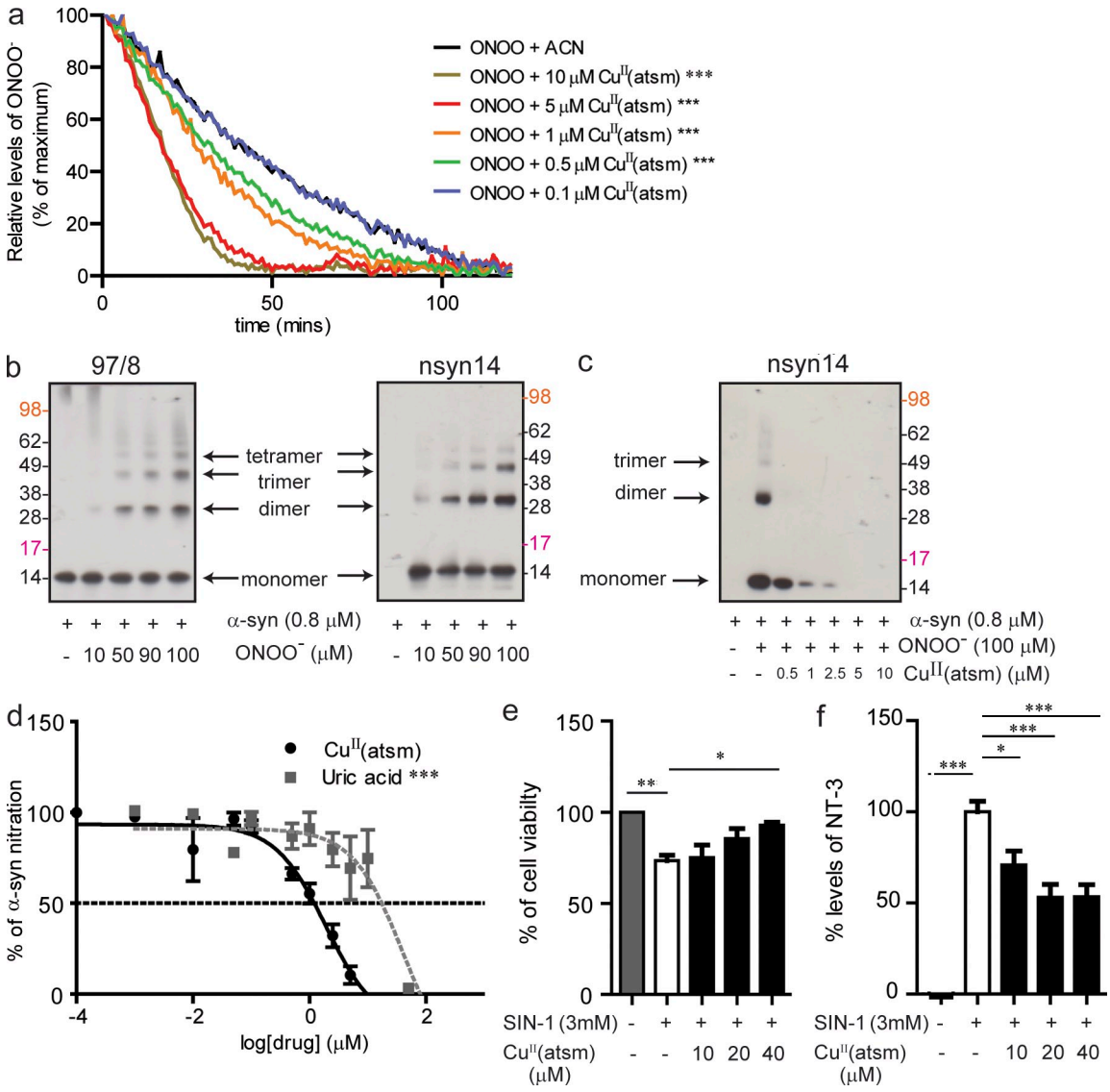

Figure 1. Cu^{II}(atsm) inhibits $ONOO^-$–induced α-synuclein and cell toxicity. (a) Effect of Cu^{II}(atsm) on the breakdown of $ONOO^-$ (500 μM, 302 nm absorbance; CAN, acetonitrile). (b) Effect of increasing concentrations of $ONOO^-$ on the formation of nitrated α-synuclein oligomers as detected by Western blot using Ab 97/8 (B, left), which detects total α-synuclein, and nsyn14 (B, right), an antibody that specifically detects nitrated α-synuclein. (c) Western blotting with the nsyn14 antibody demonstrates the effect of Cu^{II}(atsm) on $ONOO^-$-induced nitration of α-synuclein. (d) ELISA using the nsyn14 antibody showing the effect of Cu^{II}(atsm) (IC_{50} of 1 μM) on inhibiting $ONOO^-$-induced nitration of α-synuclein compared with uric acid (IC_{50} of 63 μM), an endogenous $ONOO^-$ scavenger. (e) MTS cell viability assays on differentiated SH-SY5Y cells after treatment with Cu^{II}(atsm) and SIN-1–induced cell toxicity. (f) 3-NT levels in the cell media after Cu^{II}(atsm) treatment (as detected by ELISA). For a and d, data are representative of three separate experiments and expressed as mean ± SEM; for statistical analysis, two-way ANOVA was performed with a Bonferroni post-hoc analysis. For e and f, data are representative of three separate experiments and expressed as means ± SEM; for statistical analysis, one-way ANOVA was performed with a Dunnett post-hoc analysis comparing all groups to SIN-1–exposed untreated cells. *, $P < 0.05$; **, $P < 0.01$; ***, $P < 0.001$.

SIN-1 to mimic nitrosative stress. SIN-1 reacts to spontaneously release NO and O_2^- in aqueous environments and form $ONOO^-$ (Feelisch et al., 1989). Treatment of the cells with SIN-1 for 2 h resulted in a 27% ($P < 0.01$) decrease in cell viability, as well as increased nitrotyrosine levels ($P < 0.001$; Fig. 1, e and f), this is consistent with published results (Trackey et al., 2001). Pretreatment with Cu^{II}(atsm) resulted in a dose-dependent rescue of cell loss and reduction in nitrotyrosine levels (Fig. 1, e and f). Cu^{II}(atsm) at 40 μM resulted in a 26% increase ($P < 0.05$) in cell viability and a 51% reduction ($P < 0.001$) in nitrotyrosine (3-NT) levels (Fig. 1, e and f). It seems that 50% reduction of 3-NT levels was sufficient to confer 100% protection. This is probably caused by the fact that cells can cope with a certain level of nitrosative stress and that a threshold of damage needs to be attained before toxic effects are evident; a reduction in ∼50% of 3-NT levels was therefore sufficient to afford maximum protection.

We also tested whether Cu^{II}(atsm) could rescue $ONOO^-$-mediated toxicity in a posttreatment paradigm. Cu^{II}(atsm) was added to cell culture 5 min after SIN-1, and no protective effect was observed (unpublished data). These data are consistent with Cu^{II}(atsm) having the ability to inhibit $ONOO^-$-mediated toxicity in cell culture but having no effect at inhibiting the downstream toxicity of the modified proteins.

Cu^{II}(atsm)is orally bioavailable in rats and mice

The oral bioavailability of Cu^{II}(atsm) was determined in a rat pharmacokinetic study, and a subsequent plasma and brain exposure study was performed in mice to support the in vivo efficacy studies. After oral administration of a single 20 mg/kg dose in male Sprague Dawley rats, Cu^{II}(atsm) exhibited prolonged absorption (C_{max}, 488.1 ± 67.0 ng/ml; T_{max}, 10 h), an elimination half-life of 3.1 ± 0.4 h, and an apparent oral bioavailability of 53 ± 5% (unpublished data). In C57BL/6 mice after a single oral dose of 30 mg/kg, concentrations of Cu^{II}(atsm) in plasma (C_{max}, 591 ± 203 ng/ml; T_{max}, 60 min) remained above the analytical limit of quantitation (5 ng/ml) for the duration of the 24-h sampling period and the apparent elimination half-life was ∼3.3 h (unpublished data). Measurable concentrations of Cu^{II}(atsm) were also observed in brain (C_{max}, 198 ± 61 ng/ml; T_{max}, 120 min), and concentrations remained above the limit of quantitation (10 ng/g) up to 6 h after dose (unpublished data). Based on the ratio of the area under the brain and plasma concentration time profiles up to 6 h after dose ($AUC_{0\text{-}6h}$), the brain/plasma ratio was 0.32. Based on the C_{max} levels of Cu^{II}(atsm), the maximum concentration of the compound in the brain is ∼0.6 μM.

Cu^{II}(atsm) rescued dopaminergic cell loss in multiple PD mice models

MPTP is a neurotoxin that destroys dopaminergic neurons in the SN, thereby causing PD-like symptoms such as cell death and movement disorders (Langston et al., 1983). MPTP also causes an increase in nitrosative stress (Ferrante et al., 1999; Przedborski et al., 2003). To assess its ability to rescue this phenotype, Cu^{II}(atsm) was administered by oral gavage at 15 and 30 mg/kg to mice lesioned with MPTP. To ensure that Cu^{II}(atsm) was truly neuroprotective, and not just inhibiting the actions of the toxin, a treatment regimen was undertaken wherein administration of the drug did not begin until the toxin was metabolized and a cell death cascade had commenced (1 d after lesion for the MPTP model; Meredith et al., 2008). Therefore, the MPTP lesioning took place 1 d before commencement of drug treatment, which lasted for 20 d.

It has been previously demonstrated that MPTP is metabolized and cleared by 24 h. The active metabolite of MPTP is MPP^+. Concentration of MPP^+ reached a peak in the striatal tissue within an hour of injection and reduced by 50% within 3 h; after 24 h, MPP^+ levels were negligible (Zhang et al., 2008). Similar studies have shown that 6-hydroxydopamine (6-OHDA) takes 3 d to clear (Meredith et al., 2008). This drug administration paradigm is consistent with the recommendations of Jackson-Lewis and Przedborski (2007), and has the virtue of being more closely related to the clinical setting in that any drug treatment would only begin after onset of disease.

MPTP toxicity caused a significant (∼50%; $P < 0.001$) reduction in the number of dopaminergic neurons within the SNpc (Fig. 2 a), as determined by stereological counts of Nissl-stained SNpc. Mice treated with 15 and 30 mg/kg of Cu^{II}(atsm) had 43% ($P < 0.05$) and 61% ($P < 0.01$) increases, respectively, in the number of SNpc neurons compared with vehicle-treated MPTP-lesioned mice (Fig. 2 a). Cu^{II}(atsm) was also shown to be neuroprotective in the 6-OHDA model of PD. Here 6-OHDA, a mitochondrial toxin, is injected directly into its site of action, inducing loss of SNpc dopaminergic neurons (Blum et al., 2001). There is also evidence to suggest that nitrosative stress is evident in these lesioned mice (Henze et al., 2005). To allow for complete toxin metabolism before drug administration, the Cu^{II}(atsm) treatment regimen was started 3 d after the lesion was generated. After this washout period, the mice were treated with Cu^{II}(atsm) for 20 d. The drug-treated mice showed a 26% increase ($P < 0.05$) in the number of SNpc dopaminergic neurons (Fig. 2 b). Cu^{II}(atsm) treatment had no effect on the cell numbers of nonlesioned wild-type mice (Fig. 2 a).

The toxic lesion models lack the overt α-synucleinopathy associated with PD. For this reason, Cu^{II}(atsm) was also evaluated in transgenic (tg) mice overexpressing human A53T (hA53T) mutant α-synuclein, with and without MPTP lesions. Nitrosative stress has been reported in these tg mice (Martin et al., 2006). At 7–8 mo, these tg mice had a 24% reduction ($P < 0.001$) in nigral cells compared with the wild-type control mice (Fig. 2 c), as determined by stereological cell counting. Treatment with Cu^{II}(atsm) at 30 mg/kg in the hA53T α-synuclein tg mice resulted in a significant 14% increase ($P < 0.05$) in total nigral cells (Fig. 2 c). Cu^{II}(atsm) was also tested in the hA53T tg mice lesioned with MPTP. Lesioning resulted in a 35% reduction of dopaminergic neurons compared with unlesioned littermates (Fig. 2 c). Treatment led to a significant rescue (15% increase; $P < 0.05$) of SNpc neurons (Fig. 2 c).

Cu^{II}(atsm) rescued motor impairment in PD mice

The defining clinical characteristics of PD are impairments in motor function, therefore treatments must alleviate these symptoms. Motor function in the MPTP-lesioned and tg models was evaluated by the pole test, which assesses sequential coordinated movements (Ogawa et al., 1985). The ability of an animal to undertake this task is determined by the time the animal takes to turn their body 180 degrees (T_{turn}) and total time to descend the pole (T_{total}). MPTP lesioning led to a significant decrease in motor function with increases in T_{turn} from 1.6 ± 0.4 to 3.9 ± 0.5 s ($P < 0.001$) and T_{total} from 5.1 ± 0.4 to 7.2 ± 0.6 s ($P < 0.05$; Fig. 3, a and b). These results are consistent with a previous study (Ogawa et al., 1987). Mice administered Cu^{II}(atsm) at 30 mg/kg showed significantly faster T_{turn} and T_{total} by 1.5 ($P < 0.05$) and 2.2 s ($P < 0.01$), respectively (Fig. 3, a and b), indicating improved motor function. Treatment at 15 mg/kg also resulted in a decrease of T_{turn} and T_{total} times, but these did not reach statistical significance. Cu^{II}(atsm) treatment had no effect on the motor performance of nonlesioned wild-type mice (Fig. 3, a and b).

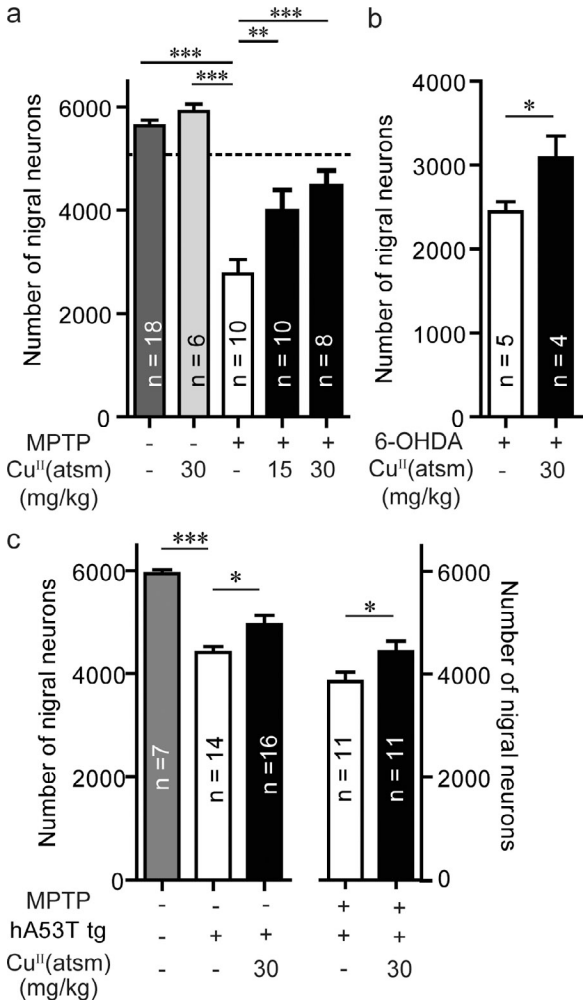

Figure 2. Cu^{II}(atsm) is neuroprotective in multiple animal models of PD. (a) C57BL/6 mice were lesioned with MPTP (40 mg/kg i.p.). The SNpc count (dotted line) was determined 24 h after MPTP lesioning (when drug treatment commenced). Effect of treatment with Cu^{II}(atsm) at both 15 and 30 mg/kg on the survival of SNpc dopaminergic neurons 20 d after lesioning. (b) C57BL/6 mice were lesioned unilaterally with 6-OHDA (intranigral dose). Effect of treatment with 30 mg/kg of Cu^{II}(atsm) on the survival of SNpc dopaminergic neurons. (c) Effect of Cu^{II}(atsm) (30 mg/kg) treatment of mice overexpressing human A53T (hA53T) α-synuclein, either nonlesioned or lesioned with MPTP on the survival of SNpc dopaminergic neurons. All data are expressed as mean ± SEM; for statistical analysis, one-way ANOVA was performed with a Dunnett post-doc analysis for multisample testing using untreated MPTP-lesioned mice (a), hA53T tg untreated or MPTP-lesioned untreated hA53T tg mice (c), and Student's *t* test for two-sample testing (b) as controls. *, $P < 0.05$; **, $P < 0.01$; ***, $P < 0.001$.

The hA53T tg model has been previously reported to lack a motor phenotype in the rotarod task at 7 mo of age (Giasson et al., 2002), and we also did not observe any impairment in this task (unpublished data). However, when tested using the pole test, these animals did exhibit significant motor dysfunctions, with the hA53T α-synuclein mutant mice taking longer to turn (2.8 ± 2.2 vs. 1.3 ± 0.5 s, respectively; $P < 0.05$) and descend the pole (7.9 ± 25.8 vs. 4.0 ± 1.0 s; $P < 0.05$) compared with the wild-type control mice (unpublished data). Treatment of the hA53T α-synuclein tg mice with Cu^{II}(atsm) was able to improve the ability of mice to perform in the pole test (T_{turn}, 1.1 ± 0.3 vs. 3.9 ± 0.5 s; Fig. 3 c; $P < 0.05$). A trend toward improvement in T_{total} times was observed but was not statistically significant (Fig. 3 d). In the hA53T tg mice lesioned with MPTP, Cu^{II}(atsm) treatment also improved motor function, as they were able to turn (1.2 ± 0.1 vs. 2.4 ± 0.4 s; Fig. 3 c, $P < 0.01$) and descend (3.9 ± 0.2 vs. 6.1 ± 0.8 s; Fig. 3 d; $P < 0.01$) the pole quicker than the corresponding vehicle-treated MPTP-lesioned tg mice. This represented a 49% improvement in T_{turn} and 37% improvement in T_{total} upon treatment.

In the 6-OHDA model, the induced toxic lesion is unilateral, and therefore the motor dysfunction manifests itself by the animal exhibiting rotational motor behavior after administration of amphetamine (Stanic et al., 2003a). Cu^{II}(atsm) treatment resulted in a reduction in rotational behavior by 45% compared with controls ($P < 0.05$; Fig. 3 e), indicating that amphetamine-stimulated dopamine release was occurring equally on both sides of the brain, which is consistent with dopamine metabolism on the lesioned side of the brain being rescued.

Cu^{II}(atsm) rescued dopamine metabolism in MPTP-lesioned mice

Perturbation of the dopaminergic system leads to inhibition of motor function. To assess whether the observed improvements in motor function were caused by alterations in dopamine metabolism, levels of striatum dopamine, tyrosine hydroxylase (TH), and vesicular monoamine transporter 2 (VMAT2) proteins were measured.

TH is involved in dopamine biosynthesis and is rate limiting in dopamine production; consistent with previous studies, MPTP lesioning resulted in significant reductions ($P < 0.05$) in TH immunoreactivity in the SNpc (Fig. 4, a and b)

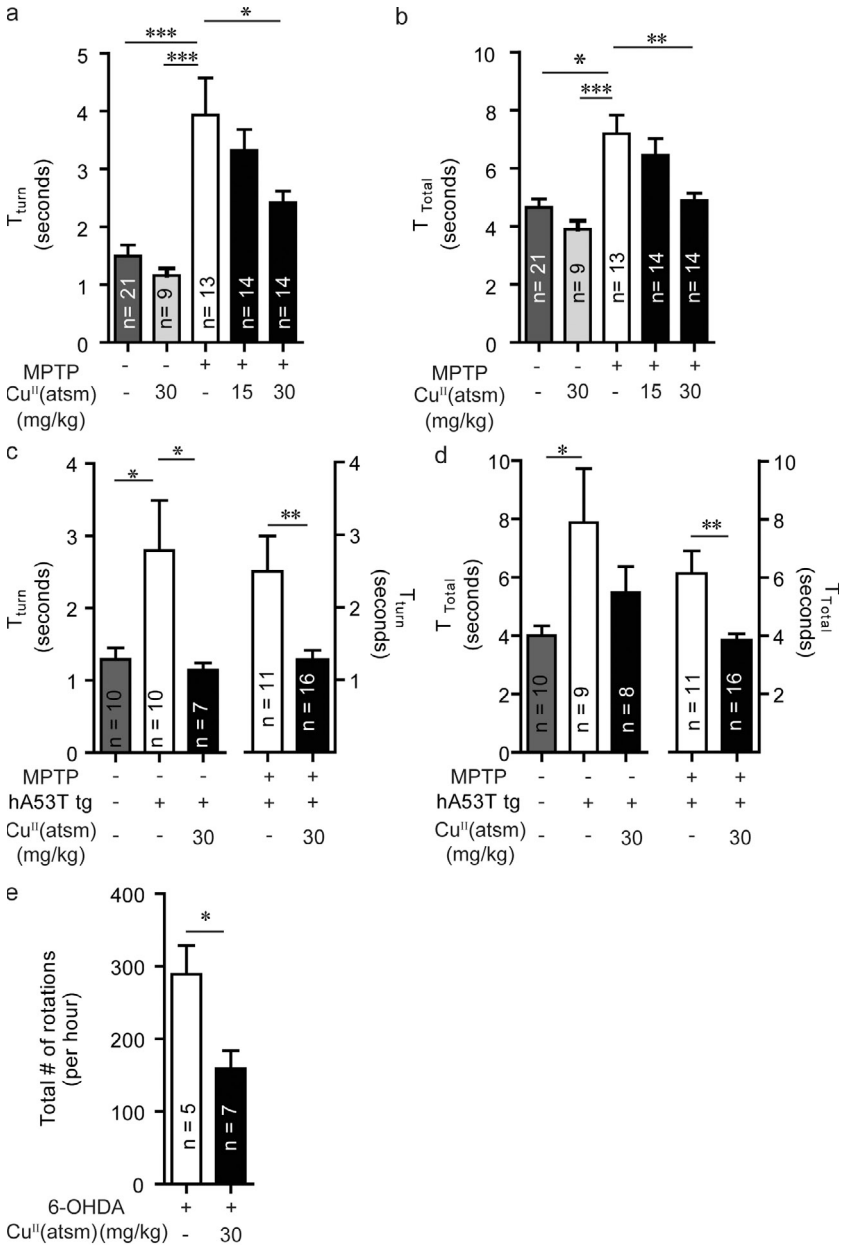

Figure 3. Cu^{II}(atsm) rescues motor impairment in multiple animal models of PD. (a and b) A pole test, which assesses sequential coordinated movement, was performed on MPTP wild-type mice after Cu^{II}(atsm) treatment. The ability of an animal to undertake this task is determined by the time the animal takes to turn their body 180 degrees (T_{turn}; a) and total time to descend the pole (T_{total}; B). (c and d) Cu^{II}(atsm) treatment effects on the T_{turn} in both unlesioned and MPTP-lesioned hA53T α-synuclein tg mice. Differences in T_{total} times were only significant for MPTP-lesioned tg, but not in the nonlesioned tg mice. (e) Effects of Cu^{II}(atsm) on the amount of amphetamine-induced rotations in 6-OHDA–lesioned mice. All data are expressed as mean ± SEM; for statistical analysis, one-way ANOVA was performed with a Dunnett post-doc analysis for multisample testing using untreated MPTP-lesioned mice (a and b), untreated hA53T tg mice (c and d), and Student's *t* test for two-sample testing (c and e) as controls. *, $P < 0.05$; **, $P < 0.01$; ***, $P < 0.001$.

and dopamine levels (Fig. 4 f; Kastner et al., 1993). Probing TH levels by Western blot showed a 37% decrease ($P < 0.01$) compared with nonlesioned mice (Fig. 4, c and d). Treatment of MPTP-lesioned mice with either 15 or 30 mg/kg Cu^{II}(atsm) increased immunostaining of TH in SNpc (Fig. 4, a and b). This result was confirmed by Western blot with 42% ($P < 0.05$) and 45% ($P < 0.05$) respective increases in the TH levels observed (Fig. 4, c and d). Furthermore, quantitative real-time PCR (qPCR) analysis of SNpc samples from these animals also demonstrated a significant decrease in TH mRNA transcript levels after lesioning by MPTP ($P < 0.05$) that was rescued by Cu^{II}(atsm) treatment ($P < 0.01$; Fig. 4 e). Consistent with increased TH levels, treatment with 30 mg/kg Cu^{II}(atsm) increased dopamine levels by 122% compared with untreated MPTP-lesioned animals (Fig. 4 f; $P < 0.05$).

VMAT2 is found on synaptic vesicles within the nerve terminals of DA synapses and functions to package dopamine from the cytoplasm into synaptic vesicles (Kanner and Schuldiner, 1987), thereby protecting it from degradation (Caudle et al., 2008). VMAT2 levels were measured in 3–4-mo-old mice lesioned with MPTP. A small but significant increase ($P < 0.05$) was observed upon treatment with 15 and 30 mg/kg Cu^{II}(atsm) (13 and 12%, respectively; Fig. 5 a). We also monitored VMAT2 levels in older (18 mo) mice by Western blot and microPET imaging, which used the radioactive VMAT2-specific ligand ^{18}F-AV133 (Hefti et al., 2010). This particular ligand has been shown to specifically detect the loss of dopaminergic synaptic terminals observed in PD and is being evaluated as a potential diagnostic tool (Wang et al., 2010). In these animals, MPTP lesioning led to a 19.5% reduction ($P < 0.05$) in ligand binding compared with vehicle control mice (Fig. 5, b and c), treatment with 30 mg/kg Cu^{II}(atsm) led to a 142% increase ($P < 0.001$) in ligand binding in the MPTP-lesioned mice when compared with vehicle control lesioned mice (Fig. 5, b and c). Although treatment led to an increase in ^{18}F-AV133 binding, the limited spatial resolution of the microPET images does not allow discrimination of regional binding of ^{18}F-AV133 in the mouse brain. The increase in VMAT2 levels were mapped by Western blot to the striatum, where Cu^{II}(atsm) treatment led to a 60% increase in VMAT2 protein levels ($P < 0.05$; Fig. 5, d and e). qPCR analysis of SNpc samples showed a decrease in VMAT2 transcripts in MPTP-lesioned animals ($P < 0.001$,) and levels were restored to those similar to the wild-type animals after Cu^{II}(atsm) treatment ($P < 0.01$; Fig. 5 f). To ensure that there was no interaction between Cu^{II}(atsm) and AV133, we measured the

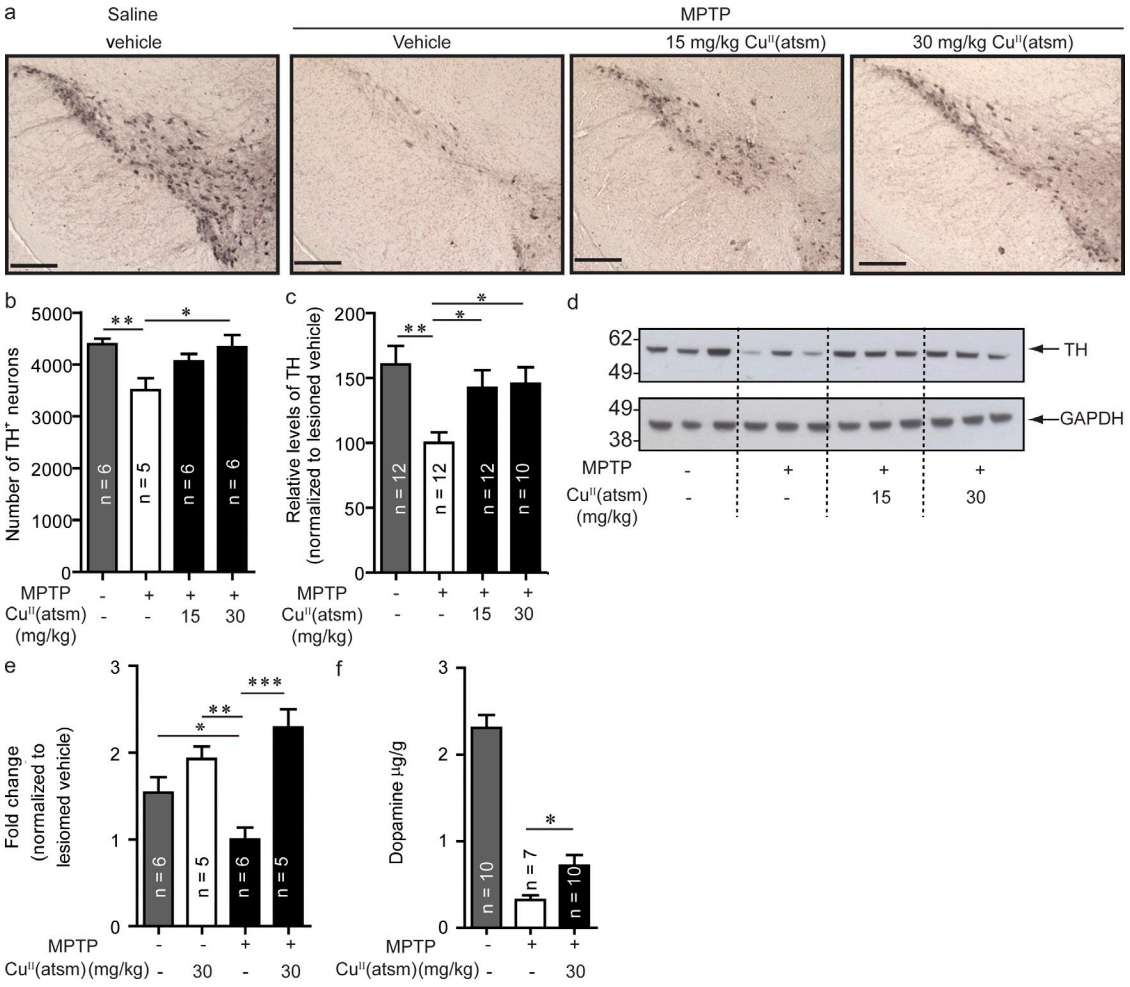

Figure 4. Cu^{II}(atsm) treatment increases TH and dopamine. (a) Sections of SNpc stained for TH from unlesioned and MPTP-lesioned mice treated with vehicle, 15 mg/kg Cu^{II}(atsm), or 30 mg/kg Cu^{II}(atsm). Results were confirmed by stereological counting (b) and Western blotting (c and d). (e) TH results were also confirmed by qPCR. (f) Dopamine levels in Cu^{II}(atsm)-treated lesioned animals compared with control lesioned animals. Dopamine levels are expressed relative to tissue weight. All data are expressed as mean ± SEM; for statistical analysis, one-way ANOVA was performed with a Dunnett post-hoc analysis for multisample testing using MPTP-lesioned untreated mice as controls. *, $P < 0.05$; **, $P < 0.01$; ***, $P < 0001$. Bars, 250 µm.

fluorescent signal of cold unlabeled AV133 (excitation at 295 nm; emission at 320 nm) in the presence of Cu^{II}(atsm) (unpublished data). If there is any significant interaction, the paramagnetic Cu^{II} in Cu^{II}(atsm) should quench the fluorescence of AV133. No change in either intensity or wavelength of (1 µM) AV-133 fluorescent was observed in the presence of Cu^{II}(atsm) of up 2 µM.

Cu^{II}(atsm) reduced levels of α-synuclein dimer in MPTP-treated mice

Recently, it has been suggested that small, soluble oligomers of α-synuclein are a likely cause of toxicity (Kazantsev and Kolchinsky, 2008). Treatment with Cu^{II}(atsm) caused a reduction in α-synuclein dimers in both the MPTP-lesioned wild-type (to 76% of control-treated, $P < 0.01$; Fig. 6, b and c) and MPTP-lesioned hA53T α-synuclein tg mice (to 83% of control-treated, $P < 0.05$; Fig. 6, e and f). Whereas no changes in monomer levels were seen in MPTP-lesioned wild-type mice (Fig. 6, a and c), there was a 12% reduction in monomer levels in MPTP-lesioned hA53T tg mice ($P < 0.05$; Fig. 6, d and f). Treatment with Cu^{II}(atsm) did not lead to any significant differences compared with vehicle treatment in α-synuclein levels of hA53T α-synuclein tg mice that were not MPTP-lesioned (unpublished data).

To investigate the effect of MPTP lesioning on expression of α-synuclein at the transcriptional level, we performed qPCR using gene-specific SNCA primers (Fig. 6 g). Interestingly, there was a down-regulation of SNCA gene transcription in MPTP-lesioned WT mice ($P < 0.05$), suggesting posttranslational modification and aggregation of α-synuclein are responsible for the increased protein levels. Upon Cu^{II}(atsm) treatment, SNCA gene regulation recovered to levels of unlesioned WT mice.

Cu^{II}(atsm) improved memory function in hA53T α-synuclein tg mice

In addition to exhibiting motor dysfunction, the hA53T mice showed memory impairments. In the novel object recognition

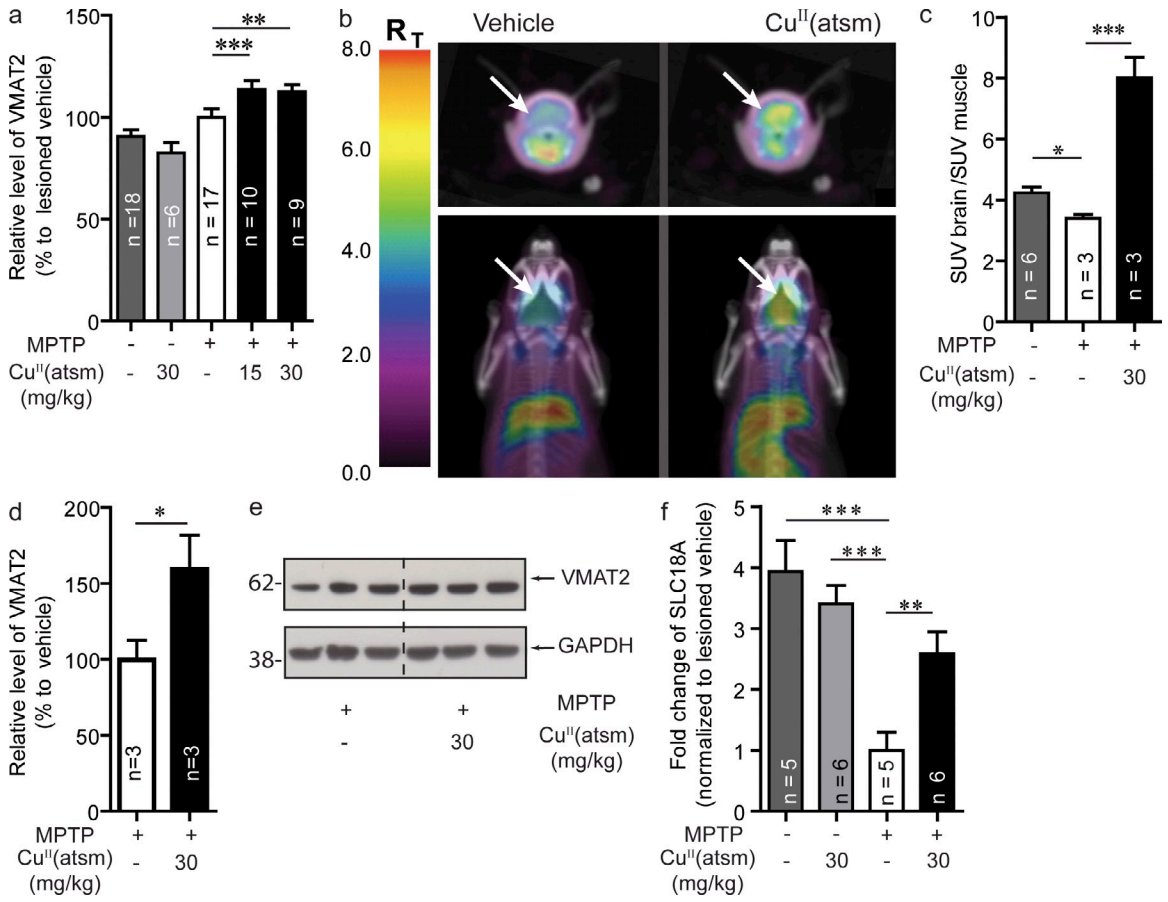

Figure 5. Cu^{II}(atsm) increases VMAT2 levels in MPTP-lesioned WT mice. (a) VMAT2 levels in young WT (4-mo-old) mice lesioned with MPTP after Cu^{II}(atsm) treatment at both 15 and 30 mg/kg doses. (b and c) VMAT2 levels were determined using the specific VMAT2 radioligand ^{18}F-AV133 and microPET imaging in older mice lesioned with MPTP (SUV, standardized uptake value). (d and e) These results were confirmed by Western blot analysis in the striatum. (f) VMAT2 gene (SLC18A) expression after lesioning and Cu^{II}(atsm) treatment. All data are expressed as mean ± SEM; for statistical analysis, one-way ANOVA was performed with a Dunnett post-hoc analysis for multi-sample testing using as controls MPTP-lesioned untreated mice (a, c, and f) and Student's *t* test for two-sample testing (d) as controls. *, $P < 0.05$; **, $P < 0.01$; ***, $P < 0.001$.

(NOR) test where memory is assessed by measuring the amount of interaction mice have with a novel object as compared with a familiar one (Ennaceur and Delacour, 1988), the tg mice interacted with novel objects at a lower frequency than wild-type control mice ($P < 0.05$; unpublished data). Consistent with this behavioral effect, the mutant mice had a 31% reduction in synaptophysin levels in the striatum ($P < 0.01$; unpublished data). Cu^{II}(atsm) treatment resulted in improved cognitive performance for these mice, with a 73% ($P < 0.05$) increase in interactions with the novel object compared with vehicle-treated mice (Fig. 7 a). Similarly, Cu^{II}(atsm) treatment resulted in an improved performance in the Y-maze test, with vehicle-treated mice having a mean 30% novel arm entries indicative of memory impairment (Fig. 7 b). Treated mice had a significantly higher mean of 42% novel arm entries ($P < 0.05$). Cu^{II}(atsm) treatment resulted in a 31% increase in synaptophysin levels as compared with vehicle-treated tg mice ($P < 0.01$; Fig. 7, c and d). This was confirmed by the increase in immunostaining of synaptophysin in the striatum of hA53T tg mice treated with either vehicle or Cu^{II}(atsm) (Fig. 7, e–g).

DISCUSSION

Current therapeutic strategies for PD, designed to replace deficits in dopamine metabolism, do not address the underlying disease processes, and therefore give only symptomatic relief. With an aging population and a rising prevalence of disease, there is an urgent need to identify new compounds capable of acting as effective disease-modifying therapeutic agents for PD. The disease is characterized by a progressive loss of neurons within the SNpc, a breakdown in dopamine metabolism resulting in impaired motor function and the deposition of misfolded α-synuclein into Lewy bodies. Therefore, a disease modifying treatment for PD ideally should be neuroprotective (i.e., inhibit cell dysfunction and subsequent death); normalize dopamine metabolism to correct the overt motor symptoms associated with the disease and reduce synucleinopathy.

Unfortunately, the identification of effective therapies for PD has been complicated by the lack of an effective animal model that fully recapitulates Parkinsonism. To date, there are numerous animal models, ranging from toxins that induce dopaminergic neuronal loss to tg models that carry the same

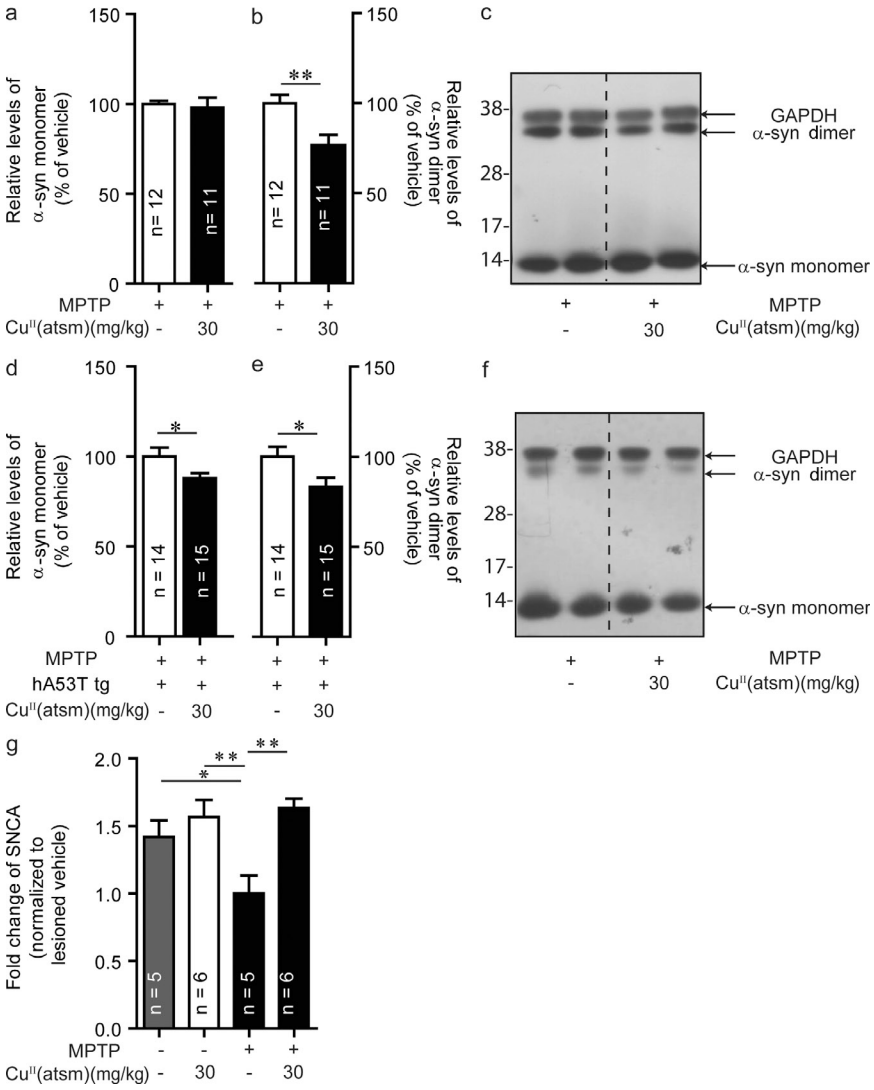

Figure 6. Cu^{II}(atsm) decreases levels of α-synuclein in the SNpc. (a–c) Effect of Cu^{II}(atsm) treatment on α-synuclein levels in MPTP-lesioned WT mice. (d–f) α-Synuclein monomer and dimer levels after treatment of hA53T α-synuclein tg mice lesioned with MPTP. (g) α-Synuclein gene (SNCA) at the transcriptional level in MPTP-lesioned WT mice and after Cu^{II}(atsm) treatment. All data are expressed as mean ± SEM; for statistical analysis, one-way ANOVA was performed with a Dunnett post-doc analysis for multisample testing (g) and Student's *t* test for 2 sample testing (a, b, d, and e). *, $P < 0.05$; **, $P < 0.01$.

genetic mutations as familial PD patients (Maries et al., 2003; Terzioglu and Galter, 2008; Meredith et al., 2008). Although each model represents different aspects of PD, none of these models manifest the full spectrum of PD pathology.

To overcome this problem the therapeutic potential of Cu^{II}(atsm) was tested in four different animal models. Two of these involved initiating a cascade of cell death within the SNpc by administering the neurotoxins MPTP or 6-OHDA, these models are able to induce cell death cascades and deficits in motor function characteristic of PD (Meredith et al., 2008). To ensure that drug effects are truly neuroprotective and not just inhibiting the actions of the toxins, we undertook a treatment regimen whereby administration of the drug did not begin until the toxin was metabolized and cell death had commenced. The ability to differentiate whether compounds impair toxin metabolism rather than affecting the underlying cell death cascade is critical. Compounds that have been reported to have neuroprotective properties in animal studies have failed in human clinical studies (LeWitt, 2004). A likely reason for this is that, to date, compounds have been primarily tested in a prelesion treatment paradigm (i.e., the drug is administered before the toxin). One example of this is CEP1347, a mixed lineage kinase inhibitor. Saporito et al. (1999) reported that this compound was only effective when pretreated 6 h before MPTP lesion without any effect when dosage was commenced after lesion (7 d). Despite this, the compound was taken forward into two clinical studies and, unsurprisingly, showed no effect in either trial (Parkinson Study Group, 2004; Parkinson Study Group PRECEPT Investigators, 2007). Therefore, to avoid a scenario where the drug inhibits the toxin rather than rescuing the cell death cascade, Cu^{II}(atsm) treatment only commenced after MPTP and 6-OHDA toxins were cleared.

MPTP lesioning initiated a cell death cascade, and after 24 h the nigral cell count within the SNpc was reduced by 10% (unpublished data). It is at this point that drug administration was started, and it is the ability of the drug to rescue the subsequent cell death that we have assessed. Cu^{II}(atsm) treatment resulted in significantly higher nigral cell counts (Fig. 2) in both models, and this was accompanied by improved motor performance (Fig. 3) in both models. Treatment also led to an increase in TH-positive neurons in the substantia nigra (Fig. 4, a and b), indicating that the neuroprotective effects seen in the more general cell counting as detected by Nissl staining also applied to the dopaminergic neurons within the SNpc. The increased levels of TH were confirmed by Western blot and qPCR analysis (Fig. 4). The higher TH levels should result in increased dopamine production, as we observed (Fig. 4 f). The level of dopamine increase was, however, not proportional to the level of motor improvement. One possible explanation for this is that although the TH-positive cells are alive they are not yet fully recovered from the effects of the toxin because of the relatively short treatment time. Nevertheless, the levels of dopamine doubled after drug treatment, although they were not fully restored to unlesioned levels. This doubling of

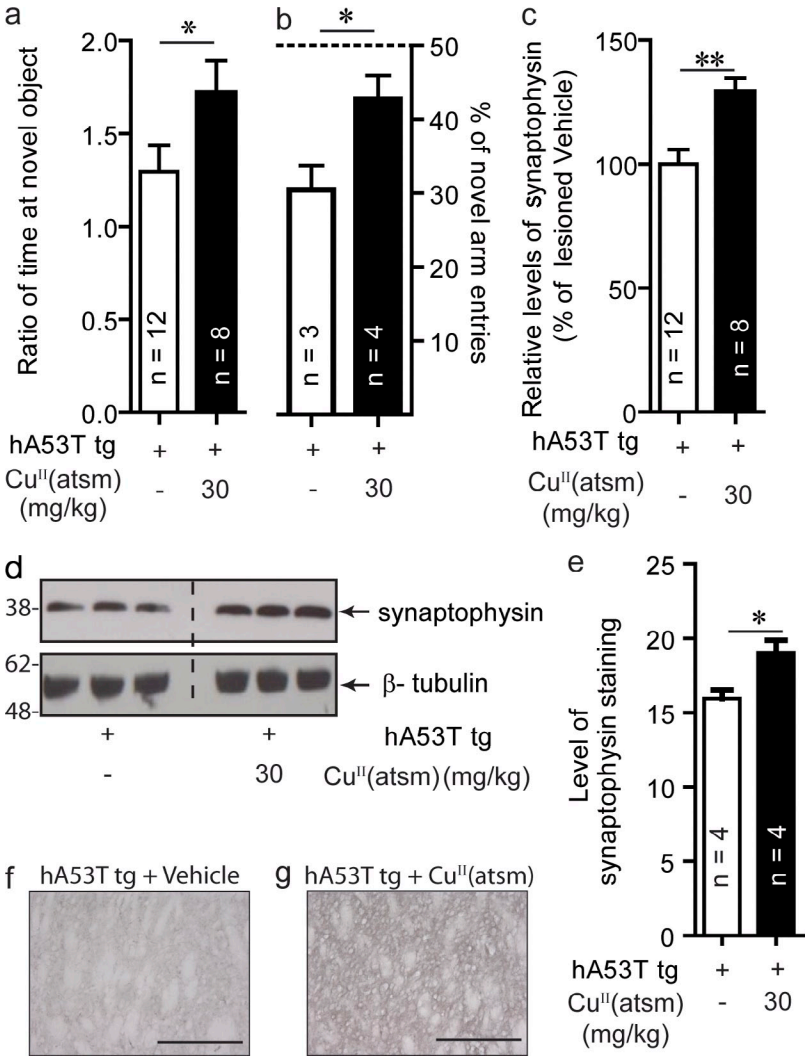

Figure 7. Cu^{II}(atsm) rescues cognitive function in hA53T α-synuclein tg mice. Mice overexpressing human A53T α-synuclein were treated with 30 mg/kg of Cu^{II}(atsm) for 20 d beginning at the age of 7 mo. (a) Cognitive performance as tested in a NOR test and in a Y-maze test (b). (c and d) Synaptophysin levels in the striatum as measured by Western blotting. (e–g) Immunoreactivity of synaptophysin in the striatum of hA53T tg mice treated with either vehicle or Cu^{II}(atsm). Bars, 250 µm. All data are expressed as mean ± SEM; for statistical analysis, Student's *t* test for 2 sample testing was used. *, $P < 0.05$; **, $P < 0.01$.

dopamine levels is probably sufficient to improve motor functions, as there is some level of dopamine redundancy. Consistent with this notion, PD motor symptoms do not manifest until ∼80% of neurons are lost (Pakkenberg et al., 1991). Furthermore, treatment also increases levels of VMAT2 (Fig. 5), the protein responsible for packaging the dopamine into vesicles. This increase should have the effect of ensuring the dopamine that is present is more efficiently used. The amphetamine challenge given to test the rotation behavior of the 6-OHDA–lesioned mice is also a measure of dopamine metabolism, as amphetamine stimulates the release of dopamine-inducing hyperactivity. Treatment-induced reduction in rotational behavior (Fig. 3 e) indicated that amphetamine-stimulated dopamine release was occurring equally on both sides of the brain, which is consistent with dopamine metabolism on the lesioned side of the brain being rescued.

α-Synuclein has been implicated in the pathology of PD, and for this reason tg mice overexpressing human A53T human α-synuclein were also investigated. Although initial studies (Giasson et al., 2002; Lee et al., 2002; Martin et al., 2006) suggested that this model more closely resembled a motor neuron disease rather than PD because of the lack of pathology in the substantia nigra, more recent data show that these tg mice do have reductions in nigral cells and increased synucleinopathy in the SNpc (Wills et al., 2011). This is consistent with our current findings showing that tg mice have both motor impairment and loss of nigral neurons (unpublished data). This apparent contradiction with earlier results is most likely a result of the methods employed, with a gross histological appearance of the SNpc being reported in the earlier studies, whereas we and Wills et al. (2011) used more rigorous stereological cell counting. Oral administration of Cu^{II}(atsm) for 20 d resulted in neuroprotective effects (Fig. 2) and improvements in motor function (Fig. 3), even when the tg mice were further impaired by MPTP lesioning. Interestingly, our data indicates that lesioning the tg mice with MPTP did not appear to have any significant additional detrimental effects on either neuronal cell counts or motor function (Fig. 2 c; and Fig. 3, c and d). There are contrary reports of the effect of MPTP on the hA53T tg mice in the literature. Whereas a study by Yu et al. (2008) reported that there was increased susceptibility of A53T mice to MPTP, Dong et al. (2002) reported that A53T tg mice did not have increased vulnerability to MPTP. This contradictory result may arise from how the transgene is expressed in the brains of mice. Yu et al. (2008) used mice that had A53T α-synuclein transgene promoted by TH, whereas Dong et al. (2002) used rAAV-mediated gene transfer to transfect the transgene. In addition, Yu et al. (2008) examined the MPTP effects on the A53T mice 5 d after lesion, whereas Dong et al. (2002) examined the effects after 5 wk. This indicates that although the A53T mice may be more susceptible to a MPTP insult in the short term, there might be compensatory mechanisms that allow it to tolerate the initial insult of the toxin over a longer period of time.

Approximately 30% of PD subjects suffer from cognitive impairment, a syndrome known as PD with dementia (Weintraub et al., 2008). In this study, the hA53T α-synuclein tg mice were shown to be cognitively impaired, as they performed poorly in both NOR and Y-maze tests (unpublished data). The cognitive

impairments of these hA53T mice observed in this study is consistent with other studies showing that A53T mice models have impaired cognition (Lim et al., 2011), as have other models overexpressing mutant human α-synuclein, e.g., the hA30P tg mice (Freichel et al., 2007). Treatment with Cu^{II}(atsm) led to significantly improved performance in both NOR and Y-maze tests (Fig. 7, a and b). Synaptophysin levels are consistent with the behavioral results with lower levels observed in the tg mice, implying impaired synaptic health (not depicted), and increased levels upon treatment, suggesting improved synaptic health (Fig. 7, c and d).

We initially identified Cu^{II}(atsm) as a potential therapeutic candidate because of its ability to inhibit the actions of $ONOO^-$ (Fig. 1), which has previously been implicated in PD pathophysiology. α-Synuclein will react with $ONOO^-$ to form toxic aggregates, and Yu et al. (2010) have recently shown that when injected into the brains of rats these aggregates recapitulate many of the features of PD, including progressive cell loss, Lewy body–like deposits, disruption to dopamine metabolism, and motor dysfunction. In vitro, Cu^{II}(atsm) only inhibits α-synuclein aggregation induced by $ONOO^-$ (Fig. 1); it does not inhibit other forms of α-synuclein aggregation (not depicted). In both MPTP-lesioned animal models, we observed a reduction in α-synuclein dimers after treatment (Fig. 6), implying that in these models α-synuclein aggregation is dependent on the actions of $ONOO^-$.

Despite there being an increase in α-synuclein protein levels and oligomerization after MPTP lesioning, this is actually accompanied by a decrease in the expression of SNCA mRNA, (Fig. 6). The most likely explanation for this apparent contradiction is that α-synuclein undergoes posttranslational modifications, such as nitration, as a consequence of the lesion, and the resulting products are resistant to protein degradation. This is consistent with a study by Meredith et al. (2002) showing that in MPTP-lesioned animals, α-synuclein aggregation was temporally correlated with a reduction in gene expression and defective protein degradation. Interestingly, α-synuclein mRNA in PD patients is also down-regulated during the early stages of disease (Neystat et al., 1999). It has previously been demonstrated that nitrated α-synuclein aggregates are resistant to degradation (Przedborski et al., 2001).

Consistent with the hypothesis that nitrated α-synuclein oligomers drive toxicity, both α-synuclein (Schlüter et al., 2003) and NOS (Hantraye et al., 1996a) knockout mice are resistant to MPTP toxicity. The specificity of Cu^{II}(atsm) in inhibiting the formation of nitrated oligomeric forms of α-synuclein in vitro (Fig. 1, c and d) and the robust therapeutic benefits observed in multiple animal models after treatment (Fig. 2 and 3) suggests that aggregated nitrated α-synuclein, or nitrosative stress, may be involved in driving many of the pathological phenomena. Moreover, nitrated α-synuclein has been found to be enriched in the Lewy bodies of PD subjects (Duda et al., 2000). Perhaps the most compelling evidence that $ONOO^-$ plays a significant role in PD pathogenesis is that levels of uric acid, an endogenous scavenger of $ONOO^-$ (Hooper et al., 1998), modulates disease susceptibility. Subjects with lower levels of uric acid in the blood are associated with a higher risk of developing the disease (de Lau et al., 2005; Andreadou et al., 2009). Conversely, subjects that suffer from gout, an inflammatory disease caused by high uric acid levels, are protected against PD (Alonso et al., 2007). Cu^{II}(atsm) is a more efficient inhibitor of $ONOO^-$ than uric acid (Fig. 1 d).

$ONOO^-$ derived toxicity has been implicated in several diseases outside of PD. One such example is ALS (Beckman et al., 1993; Beckman, 2009). We recently found that Cu^{II}(atsm) was successful in rescuing the motor phenotype in a tg mouse model of ALS (the low copy mice overexpressing human G93A SOD1) in both pre- and postsymptomatic treatment regimes; it also increased survival rates (Soon et al., 2011). Moreover, Cu^{II}(atsm) was able to reduce the level of nitrosative stress and aberrant TDP-43 processing in these mice. This confirms that this compound is generally neuroprotective and a broad effective inhibitor of nitrosative stress. Apart from PD and ALS, there is scope for Cu^{II}(atsm) to be used as a therapy outside neurodegeneration, as nitrosative stress has been implicated in a range of peripheral diseases, including cardiovascular diseases (Lee et al., 2009).

We cannot rule out that some of the observed therapeutic benefits of Cu^{II}(atsm) maybe a result of the compound stimulating neurogenesis. Indeed $NO/ONOO^-$ has been implicated as having a role in neurogenesis (Contestabile, 2008). It has shown that NO is involved in promoting the survival and differentiation of neural cells via cyclic guanosine monophosphate–cAMP response element-binding (CREB) signaling, as well as S-nitrosation of nuclear proteins that favor CREB binding to its promoters on target genes (Contestabile, 2008). However, further work is required to investigate this potential mechanism of action.

Although we have examined the therapeutic potential of Cu^{II}(atsm) in PD and ALS animal models, there are other medical applications for this molecule. Cu^{II}(atsm) radiolabeled with ^{62}Cu is currently under clinical investigation as a PET imaging agent for myocardial ischemia and hypoxic imaging in malignant tumors (Lewis et al., 2001). Donnelly et al. (2012) have recently shown that the retention of Cu^{II}(atsm) in hypoxic tissue is caused by impairment of the mitochondrial electron transport chain. Mitochondrial dysfunction has been reported as an important contributor to PD pathogenesis (Schapira, 2008), and although this manuscript was in production, Ikawa et al. (2011) published a study where $^{62}Cu^{II}$(atsm) was administered to human PD patients to assess the role of oxidative stress in these patients. The results showed that the compound selectively accumulated within the striatum and, most significantly, the more advanced the disease progression the greater the accumulation of the compound. Therefore, not only is Cu^{II}(atsm) highly effective at reducing Parkinsonian symptoms in various animal models but it also accumulates in disease relevant tissue in human PD subjects.

Cu^{II}(atsm) is a small, lipophilic, orally bioavailable molecule capable of crossing the blood–brain barrier (unpublished data). No overt toxicity associated with this compound has been observed in any of the studies described in this study or in a

longer term 12-mo trial in wild-type animals. We originally identified Cu^{II}(atsm) as a potential candidate for the treatment of PD because of its ability in vitro to inhibit $ONOO^-$-mediated nitration, including the formation of α-synuclein oligomers (Fig. 1). However, this does not rule out the possibility of other neuroprotective mechanisms playing a significant role in vivo. In summary, Cu^{II}(atsm) is neuroprotective (Fig. 2), improves cognitive performance (Fig. 7), and restores motor functions (Fig. 3) through improved dopamine metabolism (Figs. 4 and 5). These results indicate this class of compound has potential not only to treat the symptoms of PD but to be an effective disease modifying therapeutic agent for PD.

MATERIALS AND METHODS

Preparation of $ONOO^-$ and nitration of α-synuclein

$ONOO^-$ was prepared as previously described (Beckman et al., 1994). Before use, $ONOO^-$ concentration was quantified spectrophotometrically, λ_{max} = 302 nm ε = 1710 $cm^{-1}M^{-1}$. Working solutions of $ONOO^-$ were then diluted from stock to 1 mM using 0.1 M NaOH before use. Cu^{II}(atsm) was made up in solutions containing dimethyl fluoride and added at varying concentrations to a mixture containing 1 μM human α-synuclein recombinant protein (in PBS, pH 7.4) before the addition of $ONOO^-$. $ONOO^-$ was then titrated into the mixture at 1–2 μl increments while shaking vigorously. The ability of Cu^{II}(atsm) and uric acid to inhibit $ONOO^-$-induced nitration of α-synuclein, was assessed by incubating the compounds at various concentrations with α-synuclein before addition of $ONOO^-$.

α-Synuclein aggregation assays

Aggregation experiments of α-synuclein in the absence and presence of dopamine and Cu^{II}(atsm) were done as previously described in (Pham et al., 2009). Lyophilized α-synuclein was dissolved in 6 M GuHCl, 10 mM Tris-HCl at pH 7.5 to a concentration of ∼400 μM. Buffer exchange was performed on a NAP-5 desalting column equilibrated in milliQ water. The eluted protein was filtered through a 0.22 μM syringe-driven filter. Samples of α-synuclein at 20 μM were incubated in the absence and presence of 100 μM dopamine and in the absence and presence of Cu^{II}(atsm), at 37°C for 16–24 h. Soluble oligomers fractions were obtained by high speed ultracentrifugation in a Beckman Coulter TL-100 ultracentrifuge at 100,000 rpm (390,880 *g*) for 20 min at 4°C. Supernatants (soluble fractions) were collect for SDS-PAGE analysis coupled with silver staining.

Thioflavin T (ThT) fluorescence measurements were used to monitor amyloid fibril formation by the α-synuclein (at 20 μM) in the absence and presence of various molar ratio of Cu^{II}(atsm) dissolved in DMSO. Samples of α-synuclein were incubated in a thermo-mixer (Eppendorf) at 37°C with continuous shaking at 1,200 rpm. At each time point (up to 360 h), 50 ml of incubated sample was added to a well of a 96-well microtiter plate containing 220 μl of 20 mM of ThT in PBS buffer. Samples were incubated for 5–10 min and fluorescence intensities were measured in a plate reader (FLUOstar Omega; BMG Labtech Pty. Ltd.) with a 440-10 nm/480-10 nm excitation/emission filter set. All ThT measurements were performed in triplicate.

Samples from longer than 360 h were used for electron microscopy analysis. Carbon-coated grids (strong-carbon 400-mesh; ProSciTech) were glow-discharged immediately before use to increase surface wetting and sample adsorption. Samples (10 μl droplets) of α-synuclein in the absence of presence of 4 μM Cu^{II}(atsm) were applied neat onto the grids for 1–2 min within 15 min of glow discharge treatment and stained twice with 5 μl drops of 1.5% uranium acetate. The grids were then air dried and examined using an FEI Tecnai F30 microscope operating at 200 kV.

NMR spectroscopy

2D [^{1}H,^{15}N] HSQC NMR performed on ^{15}N-labeled α-synuclein was performed on a Bruker-BioSpin Avance 800 MHz spectrometer equipped with a cryogenically cooled probe. All experiments were performed at 25°C, and samples were typically 0.25 mM of ^{15}N α-synuclein WT protein in 0.5 ml in 10 mM phosphate buffer, pH 7.4, with 10% D_2O/90% H_2O. For all double-resonance spectra, 2,048 complex data points were collected for each direct dimension, and 512 complex data points in the indirect dimension. All NMR data were processed using the software TOPSPIN (Bruker BioSpin AG).

Cell culture

Human neuroblastoma SH-SY5Y cells (American Type Culture Collection) were grown in DME (Invitrogen) supplemented with 20% FCS, 100 μg/ml penicillin, 100 μg/ml streptomycin, and 2 mM L-glutamine. Cells were maintained in humidified, 37°C chambers with air/CO_2 (19:1). Upon confluence, cells were plated onto 6-well plates at a density of 2×10^5 cells/well. 24 h after plating, cells were differentiated with retinoic acid (RA) by growing in media containing 1.5% FCS and 10 μM RA for 3 d; the media was then removed and replaced with fresh RA media for another 3 d of differentiation. RA-differentiated cells were further differentiated with 80 nM 12-O-tetradecanoyl-phorbol-13-acetate (TPA) in 1.5% FCS media for another 6 d, with media changed after every 3 d. Cells treated with a combination of RA and TPA have previously been shown to differentiate into cells closely resembling dopaminergic neurons (Presgraves et al., 2004).

RA/TPA-differentiated cells were preincubated with 10, 20, and 40 μM of Cu^{II}(atsm) for 5 min, and then insulted with 3 mM of SIN-1 for 90 min. MTS cell viability assays were done after this time according to the manufacturer's specifications. In addition, media were collected and cells harvested and lysed for ELISA analysis. In brief, cells were collected with PBS at room temperature, spun down, and washed again with PBS. Cells were then lysed with ice cold lysis buffer (containing 50 mM Tris, pH 7.4, 150 mM NaCl, 2 mM EDTA, 2% NP-40, and 1X protease inhibitor). Cell lysate was then spun at 10,000 *g* at 4°C. Supernatant was collected and used for ELISA analysis.

Pharmacokinetic methods

Rat pharmacokinetic studies. Cu^{II}(atsm) was administered orally by gavage (1 ml, followed by a 1-ml water rinse of the dosing apparatus) at a dose of 20 mg/kg (n = 3) or intravenously by infusion (dose volume, 0.5 ml; infusion rate, 0.05 ml/min) via an indwelling jugular vein cannula at a dose of 5 mg/kg (n = 3) to fasted, male Sprague Dawley rats aged 6–8 wk old and weighing ∼280 g. The oral formulation was a suspension (6 mg/ml Cu^{II}(atsm)) in SSV as used in the efficacy studies. The intravenous formulation was a solution (3 mg/ml Cu^{II}(atsm)) in an organic vehicle containing 20% DMSO and 80% propylene glycol. Rats were fasted overnight before dosing and food was reinstated 4 h after dose. Animals had access to water ad libitum throughout the pre- and postdose sampling period. Arterial blood samples were collected over the 24 h postdose period by a Culex Automated Blood Sampler (Bioanalytical Systems Inc.) via an indwelling carotid arterial cannula inserted under surgical anesthesia on the day before dosing. Serial blood collection was performed for individual rats up to 24 h after dose administration directly into heparinized borosilicate vials maintained at 4°C; blood samples were centrifuged and aliquots of plasma were stored frozen at −20°C until analysis by liquid chromatography-mass spectrometry (LC-MS).

Mouse pharmacokinetic and brain uptake studies. Cu^{II}(atsm) was administered orally by gavage at a dose of 30 mg/kg animal weight to male C57BL/6 mice aged 11 wk old. The formulation (7.5 mg/ml of Cu^{II}(atsm)) was prepared in standard suspension vehicle (SSV), as used in the efficacy studies. At selected time points up to 24 h after dose (n = 3 mice per time point), mice were anaesthetized with 100 mg/kg sodium pentobarbitone (Lethobarb; Jurox), and ∼500 μl of blood was withdrawn by terminal cardiac puncture and transferred to heparinized tubes. Blood samples were immediately centrifuged, and duplicate 50-μl aliquots of plasma were collected for analysis. Immediately after death, brains were blotted to remove residual blood, weighted, and placed into tubes that were snap frozen on dry-ice. Plasma and brain samples were stored frozen at −80°C until analysis by LC-MS.

Bioanalysis of plasma and brain samples. Quantitation of Cu^{II}(atsm) in plasma and brain samples was performed using LC-MS (Xevo TQ mass

spectrometer coupled to an Acquity UPLC; both from Waters). Chromatographic separation was conducted using a Supelco Ascentis Express RP Amide 50 × 2.1 mm column eluting with methanol-water gradient with 0.05% formic acid. Elution of Cu^{II}(atsm) and the internal standard, diazepam, was monitored in positive electrospray ionization multiple-reaction monitoring mode using the transition of 322.0 > 248.8 and 285.2 > 154.1, respectively. Whole brains were homogenized in three parts (by weight) of water on ice before precipitation. Cu^{II}(atsm) concentrations were quantified in plasma and brain homogenate against calibration standards prepared in blank plasma or brain homogenate, as appropriate. Both samples and standards were prepared by precipitation with acetonitrile, followed by centrifugation and analysis of the supernatant. The analytical lower limit of quantitation was 10 ng/ml in rat plasma, 5 ng/ml in mouse plasma, and 10 ng/g in mouse brain homogenate.

SOD activity measurement. The SOD activity of Cu^{II}(atsm) was assessed spectrophotometrically (Bioxytech SOD-525; OXIS International) according to the manufacturer's protocol and as previously described (Nebot et al., 1993).

Animal experiments

All methods conformed to the Australian National Health and Medical Research Council published code of practice for animal research, and experimentation was approved by a University of Melbourne Animal Ethics Committee. Rat pharmacokinetic studies were conducted in accordance with the Australian Code of Practice for the Care and Use of Animals for Scientific Purposes and were approved by the Monash Institute of Pharmaceutical Sciences Animal Ethics Committee. Sprague Dawley rats and C57BL/6 mice were purchased from the Monash Animal Services. A breeding colony of tg mice that overexpress human α-synuclein with the A53T mutation driven by the mouse prion promoter was established from previously characterized mice (Giasson et al., 2002). In addition, all studies were conducted in a blinded fashion to remove any bias associated with analysis.

MPTP lesioning of C57BL/6 mice and hA53T α-synuclein tg mice

Four doses of MPTP (Sigma-Aldrich) were injected intraperitoneally into C57BL/6 and hA53T α-synuclein tg mice (Giasson et al., 2002) at a dose of 10 mg/kg at 2-h intervals, the total dose per mice being 40 mg/kg. This dose was chosen to ensure that all mice would survive the lesioning process but still manage to get a reduction in dopaminergic neurons in the SNpc. Our previous studies have shown that this dose would elicit ∼50% reduction in nigral neurons, which is consistent with the results in this study. C57BL/6 female mice were 4-mo-old, and 7-mo-old hA53T α-synuclein (equal number male and female) were used 1 d after lesioning. Mice were treated with 15 or 30 mg/kg Cu^{II}(atsm) or SSV (NaCl, 0.9% wt/vol; carboxymethyl cellulose, 0.05% wt/vol; Benzyl alcohol, 0.05% vol/vol; Tween 80, 0.04% vol/vol) via oral gavage for 21 d. In addition to the toxin-injected mice, a cohort of mice were sham lesioned with saline, and then orally gavaged with SSV for the duration of the trial. Pole test was performed after 19 d of treatment (see Pole test). Animals were killed by an overdose of sodium pentobarbitone (100 mg/kg Lethobarb; Jurox), and perfused via the heart with cold 0.1 M PBS (Sigma-Aldrich), pH 7.4.

hA53T α-synuclein tg mice

hA53T α-synuclein tg mice and WT background controls (C57BL/6 x C3H) were 7 mo of age at the commencement of the trial. Equal numbers of males and females were used. Mice were treated with either Cu^{II}(atsm) at 30 mg/kg or vehicle (SSV) via oral gavage for 20 d. Pole test, Y-maze and NOR test were performed during the trial (see Y-maze and NOR test).

6-OHDA toxin lesioning

A partial lesion of the SN was produced in 2-mo-old C57BL/6 mice by injecting 6-OHDA (Sigma-Aldrich) into the right SN. The mice were medicated with 0.5 mg/kg atropine (Pharmacia Pty. Ltd.) and 10 mg/kg xylazine (Troy Laboratories Pty. Ltd.) before induction of anesthesia with 3–4% Isoflurane (Abbott Australasia Pty. Ltd.) carried by oxygen. Once the animals had a diminished flexor response, the anesthetic was decreased to 1.5–2.5% Isoflurane and the heads were secured in a stereotaxic frame with the bite bar 3 mm above horizontal. A solution of 1.65 mg/ml 6-OHDA was prepared with 0.2 mg/ml ascorbic acid (Sigma-Aldrich) and kept on ice until the time of injection. A 26-gauge needle attached via tubing to a 500 µl Hamilton syringe mounted in a syringe pump (Bioanalytical Systems Inc.) was inserted into the right SN through a small hole drilled through the top of the skull. The needle was left to settle for 2 min before 2 µl (2.5–3.3 mg, 1.5–1.65 mg/ml) of 6-OHDA was injected slowly (0.5 µl/min) into the right SN (anteroposterior, 3.0 mm; lateral, 1.1 mm; dorsoventral, 4.7 mm, with respect to bregma). On completion of the injection, the needle was left in place for 2 min then slowly withdrawn at a rate of 1 mm/min. After surgery, the skin was sutured, antiseptic (1% wt/wt Betadine iodine; Faulding and Company) was applied to the wound, and the mice were left in a warmed cage to recover. Paracetamol (100 mg/kg; GlaxoSmithKline) was administered in drinking water as an analgesic after surgery.

Mice commenced treatment with 30 mg/kg Cu^{II}(atsm) 3 d after lesioning. 3 d after lesioning and before commencement of treatment, amphetamine-induced rotational behavior was done to ensure that the lesion was large enough, as previously described (Stanic et al., 2003a; see Amphetamine-induced rotation). Mice were randomly assigned to a treatment group that received Cu^{II}(atsm) or sham group given vehicle for another 18 d, after which another rotational test was performed.

Amphetamine-induced rotation

This assay examines amphetamine-induced motor asymmetry (i.e., a measure of dopamine asymmetry) in animals that receive a unilateral modification to the SN neurons. The mouse is connected to the automated Rota-Count system with a cable tie (Columbus Instruments) and is allowed to acclimatize to the system for 30 min. The mouse is then injected with 5 mg/kg amphetamine, and cumulative rotations are collected for the subsequent hour. The asymmetry of the lesions will be compared by observing the direction and number of turns (Stanic et al., 2003a).

Pole test

A pole test based on a previous study (Ogawa et al., 1985), was used to assess specific motor impairments related to basal ganglion pathology. Numerous works have been published highlighting its utility (Matsuura et al., 1997; Sedelis et al., 2001; Meredith and Kang, 2006). Consistent with the sensitivity of this test, L-DOPA has been shown to reverse MPTP impairment in the pole test. The data presented in the article and the cited papers indicate that the pole test is an appropriate test for impairment of basal ganglia function. In this test, mice are assessed for their ability to coordinate and descend a pole. Hence, this test is designed to detect deficits in planning and performing motor tasks that have close association to motor and gait abnormalities seen in PD patients.

The mice were placed with the head facing up on top of a vertical rough-surfaced pole (dimensions: 50 cm in length, 1 cm diameter). The base of the pole was placed in their home cage to ensure and encourage the animal's return to a familiar environment. On the day before testing, the animals were habituated to the pole and were allowed five trials. On the day of testing, the animals had five sessions, during which they were assessed for the time it took to completely turn orientation (T_{turn}) and to descend the pole (T_{total}). The best times of the 5 trials were used for both T_{turn} and T_{total}. If the mouse had failed to turn completely or fell off the pole the default value of 60 and 120 s were given, respectively. Animals were recorded via a digital video camera on the test day. The digital video image of the mouse and stop watch was played back in slow motion, and time scores were obtained for both tasks. The best times for both the T_{turn} and T_{total} were noted and used in the statistical analysis. In this study, pole test was done after 19 d of treatment.

NOR test

After 18 d of treatment, hA53T α-synuclein tg mice were subjected to a NOR test. The NOR test was performed according to the protocol described previously (Ennaceur and Delacour, 1988), but with certain modifications. The experiments were performed in a 38 × 27 × 12 cm (length × width × height) white box with a glass cover. Before the test, mice were habituated to the test box for 15 min per day for 3 consecutive days with no objects present. On the fourth day, mice were placed in the test box and exposed to two identical objects (measuring 1.5 × 1.5 × 1.0 cm) placed in two corners (∼25 cm apart). The objects used in this study were Lego blocks. The mice were left to explore the

objects for a period of 10 min (defined as the training session). The mice were then returned to their home cage. After a waiting period of 1 h, the mice were placed in the test box again with one of the familiar objects used in the previous training session replaced with a novel object (measuring 1.5 × 1.5 × 2.0 cm). The time spent exploring each object was recorded during the subsequent 5 min period (defined as the test session). The animals were regarded to be interacting when they were facing, sniffing, biting, or standing on the object. The test box and the objects were cleaned with 70% ethanol between trials. The ratio of time spent interacting with the novel object over the time spent interacting with the familiar object was used as an index to measure memory preference.

Y-maze test

After 20 d of treatment, hA53T α-synuclein mice were subjected to a Y-maze test, with all testing performed during the light phase of the circadian cycle. The Y-maze was of uniform gray color and consisted of three arms with an angle of 120° between each arm. Each arm was 8 × 30 × 15 cm (width × length × height). The three identical arms were randomly designated start arm (always open and in which the mouse started to explore), novel arm (which was blocked during the first trial but opened during the second trial), and other arm (always open). The maze was placed in a separate room with minimal lighting, and the floor of the maze was covered with sawdust that was mixed after each individual trial to eliminate olfactory stimuli. Visual cues were placed on the walls of the maze. The Y-maze test consisted of two trials separated by a 1-h intertrial interval to assess short-term spatial recognition memory. The first trial (training) was for 10 min, and the mice were allowed to explore only two arms (starting arm and other arm). For the second trial (retention), mice were placed back in the maze in the same starting arm and allowed to explore for 5 min with free access to all three arms. Using a ceiling-mounted charge-coupled device camera, all trials were analyzed for the number of entries the mice made into each arm. Data are expressed as the percentage of novel arm entries made during the 5-min retention trial.

Histology, estimation of lesion size, and stereological cell counts

After the mice were sacrificed with an overdose of anesthetic, and then immediately perfused with cold PBS. The right hemisphere of the brain was placed in 5 ml of chilled 4% wt/vol paraformaldehyde (Sigma-Aldrich) in 0.1 M phosphate buffer overnight (4°C; Sigma-Aldrich), pH 7.4. The brains were then removed and left at 4°C overnight in 30% wt/vol sucrose (domestic grade) in PBS before being frozen and sectioned on a cryostat. C57BL/6 brains were cut coronally into 30-µm sections in a 1:3 series for the SNpc.

These sections were stained with Neutral Red (Nissl stain; Sigma-Aldrich). Before immunostaining, the frozen sections are fixed again for 5 min. This is to ensure that the brain sections are properly fixed to the glass slide. From our experience, this protocol has been robust and generated reproducible data, not only from within the laboratory but also to data generated in the literature (Finkelstein et al., 2000, 2004; Parish et al., 2001; Stanic et al., 2003a; Lee et al., 2008). The SNpc was recognized as the sheet of densely packed neurons of ∼11 × 20 µm in soma size. At the ventral margin of the SNpc, the SNp reticulate (SNpr) neurons were recognized because their soma were larger (∼20–45 mm) and less densely packed than those in the SNpc. The VTA had smaller and less densely packed cells than the SNpc, making the rostromedial border of the SNpc easy to delineate. Caudally, the medial border of the SNpc excluded the loosely scattered neurons in the medial lemniscus. SNpc nuclei from both normal and lesioned animals were examined. In each of the sections sampled, counts of SNpc neurons were made using optical dissector rules (Gundersen et al., 1988) and the nuclei of stained SNpc cells were the counting unit (Finkelstein et al., 2000). In our previously published studies, we reported only 7% of the SNpc to be nondopaminergic.

The total number of neurons in the SN was estimated using fractionator sampling (West and Gundersen, 1990; Finkelstein et al., 2000; Stanic et al., 2003b). Counts were made at regular predetermined intervals (x, 140 µm; y, 140 µm). The entire SNpc was sampled at every third section and analyzed in a series having a random offset for each brain. Stereology was performed on a series which consisted of 7–9 SNpc sections using a random first section to start. The nigral cell counts were generated from 8 sections with an meanarea sampled of 2.48×10^8 µm^3. Systematic samples of the area occupied by the nuclei were made from a random starting point. When photographing the SNpc, we attempt to obtain the same location in all of the images. We take the images at the third nerve radical. The slight variation in appearance VTA could be because of slight differences of the angle of sectioning and the variation in stain intensity. An unbiased counting frame of known area (45 µm × 35 µm) was superimposed on the image of the tissue sections using a stereological software package (Stereology Investigator 7; MBF Bioscience) using a Leica DMLB microscope (Leica).

Immunohistochemical detection of TH in mice brains

Coronal sections of the SNpc (30 µm) were used to immunostain for TH, as previously described (Stanic et al., 2003a). Sections were fixed with 4% PFA for 1 min, and then boiled in citrate buffer (10 mM + 0.05% Tween 20, pH 6.0) to increase antigen–antibody interaction. Sections were then incubated with blocking solution (0.1 M PBS, 0.3% Triton X-100 [Sigma-Aldrich], and 3% normal goat serum) for 20 min at room temperature and then overnight at room temperature with primary antibody (rabbit α-TH, Millipore, 1:3000 in 0.1M PBS, 0.3% Triton X-100, 1% normal goat serum, 1% BSA) overnight at room temperature. After washes, secondary HRP-conjugated goat α-rabbit antibody (neat; Millipore) was incubated with the sections for 3 h at room temperature. After washes, sections were reacted with cobalt and nickel-intensified diaminobenzidine (DAB; Sigma-Aldrich) for 15 min. 3.33 µl/ml hydrogen peroxide was added to the DAB solution for an additional 5 min. Rinses in 0.05% TBST (3 × 5 min) were performed between each step. Sections were counter stained with Neutral Red, and then dehydrated in a series of graded ethanol solutions (50–100%) and cleared with histolene before being coverslipped with DPX mounting medium.

Densitometry for synaptophysin immunohistochemistry of the striatum

30-µm coronal sections of the SNpc were incubated with synaptophysin antibody (Millipore) for overnight at room temperature and washed with 0.1% TBST 3 times for 2 min. Sections were then incubated with anti–mouse HRP antibody for 2 h at room temperature, and then washed with 0.1% TBST 3 times for 2 min before the addition of DAB solution and mounted with DPX. Images of the immunostained sections were taken within 48 h using a DM2500 microscope (Leica). Section was looked at under a 10× objective lens and the section with the most anterior commissure was selected. The top interior corner of the striatum was lined up with the top right hand corner of the Leica imaging screen. The lens was then changed to a 20× objective lens and an image was obtained with a DFC310FX camera and imaging software (both from Leica). The slide was moved 1.1 mm along the y axis, where another image was obtained. This was repeated for each of the samples.

ImageJ (National Institutes of Health) was used to analyze images. Each image was opened using Image J and the image colors were inverted. A reading was taken of the entire image, and a background reading was chosen from an area where there was no tissue and used to subtract from the image. This was repeated on all images. Both the image and background areas were maintained as constant. For each section, the resulting two readings were averaged and used as a value for the section. All animals were processed and imaged in parallel, with the observer blind to the group identity.

Tissue preparation for biochemical analysis

The left brain hemisphere was dissected into regions containing the striatum (caudate nucleus and putamen) and the SNpc. These fractions were homogenized using a probe sonicator in Dulbecco's PBS containing protease and phosphatase inhibitors (1:5; tissue weight in milligrams: buffer volume in microliters). Homogenates were centrifuged at 13,200 rpm for 20 min at 4°C. The supernatant was collected as the PBS soluble fraction. The resulting pellet fraction was resuspended in the same volume of homogenizing buffer and sonicated. This fraction was then collected as the PBS insoluble fraction. A BCA assay was performed on all samples to determine protein content. Samples were then diluted and made to 2 µg/µl aliquots and used for biochemical analysis.

Western blot analysis of mice brain homogenate

Brain homogenates (∼20 µg) or recombinant α-synuclein (∼1 µg) were diluted in SDS-loading buffer, reduced in β-mercaptoethanol and heated to

90°C for 5 min. Protein samples were then separated by 10% SDS-PAGE (Invitrogen) and transferred onto nitrocellulose membranes. Membranes were blocked in 5% non-fat skim milk diluted in TBS to remove nonspecific immunoreactivity. Membranes were then probed with antibodies to α-synuclein (antibody 97/8 [1:10,000; Culvenor et al., 1999] and LB509 [1:10,000; Baba et al., 1998] for total and human α-synuclein, respectively), nitrated α-synuclein nsyn14 (1:3,000; Millipore), VMAT2 (1:500; Millipore), synaptophysin (1:75,000: Millipore), and TH (1:10,000: Millipore). After three 10 min washes with 0.1% TBS/T, the immunocomplex was probed with HRP-conjugated secondary antibodies. Probed membranes were washed three times in 0.1% TBS/T for 10 min each, and the immunoreactive proteins were detected using enhanced chemiluminescence upon reaction with ECL (Millipore). All Western blot densitometry data are normalized to levels of the loading control GADPH or β-actin and expressed as percentage to vehicle levels.

Detection of 3-NT and nitrated α-synuclein by ELISA

Nitrated α-synuclein and 3-NT levels were determined by ELISA. In brief, ELISA was done at 22°C and all antibodies were prepared in 0.1% casein in 8 mM PBS (pH 7.4). Immuno 96-well plates were incubated with recombinant α-synuclein (±$ONOO^-$), cell media, cell lysate, or brain homogenate (~10 µg of protein) diluted in 100 mM carbonate buffer, pH 9.6, for 2 h at room temperature. After blocking with StabilCoat (SurModics) for 1 h and washing with PBS containing 0.1% Tween 20, the plates were incubated with either nitro-α/β-synuclein nsyn14 (mouse, 1:3,000; Millipore) or anti-tyrosine (rabbit, 1:2000; Cell Signaling Technologies) antibodies for 2 h at room temperature. Next, the plates were incubated with HRP-conjugated secondary antibodies for 1 h at room temperature. TMB substrate (GE Healthcare) was then incubated for 15 min, and the reaction was stopped after 10–15 min by addition of 10% HCl. Absorbance values was measured at 450 nm. In the case of brain homogenates, nitrated α-synuclein and 3-NT levels were normalized to protein concentration and expressed relative to the amount of SNpc dopaminergic neurons.

Dopamine measurement of mouse striatum

In brief, the right striatum was homogenized by pulse sonication in 0.4M perchloric acid (Chem Supply Co.), 0.15% sodium metabisulfite (Univar), and 0.05% ethylenediaminetetra acetic acid disodium salt (Chem Supply Co.). The homogenate was subsequently spun at 13,000 RPM at 4°C for 10 min, and the supernatant was collected for dopamine and dihydroxyphenylacetic acid (DOPAC) measurement. Analysis of dopamine and DOPAC was undertaken with HPLC coupled with electrochemical detection. In brief, 50 µl supernatant samples were injected onto a MD-150 reverse phase C18 column (ESA). The mobile phase consisted of 75 mM sodium dihydrogen phosphate, monohydrate (Sigma-Aldrich), 1.7 mM 1-octanesulfonic acid sodium salt (Sigma-Aldrich), 100 µl/l triethylamine, 25 µM EDTA (Sigma-Aldrich), 10% acetonitrile, pH 3.0. The mobile phase was filtered and degassed before being pumped through the system at 0.6 ml/min using an HPLC pump (model 584; ESA). Compounds were detected and quantified with an Coulochem III detector with conditioning cell (ESA) and microdialysis cell (ESA; E1, −150 mV; E2, +220 mV; guard cell, +250 mV). Peaks were identified by retention times set to known standards. Data were normalized for total wet weight of sample.

Gene expression analysis using qPCR

Total RNA was isolated from SNpc sections using the miRNeasy RNA kit (QIAGEN), and RNA integrity was assessed using the RNA Nano 6000 kit and the 2100 Bioanalyser (Agilent). RNA samples that had a ribosomal integrity number (RIN) of at least 7 were selected for qPCR analysis. Reverse transcription was performed on 1.2 µg of total RNA using the High Capacity cDNA Conversion kit (Applied Biosystems). qPCR was performed with RT^2 qPCR SYBR Green Real-Time PCR Assays (TH; PPM05014A, VMAT2; PPM41860A and SNCA; PPM25867E; SA Biosciences). qPCR reactions were analyzed on the StepOnePlus qPCR instrument (Applied Biosystems). For data normalization across samples, GUSB (PPM05490B; SA Biosciences) was used as an endogenous control gene. Normalization of Ct values of each gene and determination of fold differences in gene expression (normalized to lesioned mice) was calculated by the $2^{-\Delta\Delta Ct}$ method. Sample size of each group is indicated in the graphs under the respective bar area.

VMAT2 microPET imaging

Female B6C3H x HeJ mice at 18-mo-old were lesioned with MPTP. Before lesioning, baseline levels of VMAT2 were measured by microPET imaging of ^{18}F-AV-133 uptake. Mice were administered 500 µCi of ^{18}F-AV-133 via tail vein injection and imaged for 30 min after the injection. Mice were then lesioned with 4 × 10 mg/kg MPTP. Cu^{II}(atsm) treatment commenced the following day and continued for a further 21 d, upon which VMAT2 levels were reassessed by microPET imaging.

Statistical analyses

All data are presented as the means ± SEM, and we evaluated statistical differences by Student's *t* test for two-sample testing and one-way ANOVA test for multisample testing, unless otherwise stated. Post-hoc testing was done with Dunnett's test comparing to vehicle control in all circumstances. For all analyses, we considered $P < 0.05$ to be statistically significant. Sample size of each group is indicated in the graphs under the respective bar areas.

We thank Virginia M. Lee and John Q. Trojanowski for the tg mice.

This work was funded by the Australian National Health and Medical Research Council. L.W. Hung and P.J. Crouch are Melbourne Neuroscience Institute Research Fellows.

There are no commercial affiliations or competing financial interests by any authors.

Submitted: 27 October 2011
Accepted: 1 March 2012

REFERENCES

Alonso, A., L.A. Rodríguez, G. Logroscino, and M.A. Hernán. 2007. Gout and risk of Parkinson disease: a prospective study. *Neurology*. 69:1696–1700. http://dx.doi.org/10.1212/01.wnl.0000279518.10072.df

Andreadou, E., C. Nikolaou, F. Gournaras, M. Rentzos, F. Boufidou, A. Tsoutsou, C. Zournas, V. Zissimopoulos, and D. Vassilopoulos. 2009. Serum uric acid levels in patients with Parkinson's disease: their relationship to treatment and disease duration. *Clin. Neurol. Neurosurg.* 111:724–728. http://dx.doi.org/10.1016/j.clineuro.2009.06.012

Baba, M., S. Nakajo, P.H. Tu, T. Tomita, K. Nakaya, V.M. Lee, J.Q. Trojanowski, and T. Iwatsubo. 1998. Aggregation of α-synuclein in Lewy bodies of sporadic Parkinson's disease and dementia with Lewy bodies. *Am. J. Pathol.* 152:879–884.

Beckman, J.S. 2009. Understanding peroxynitrite biochemistry and its potential for treating human diseases. *Arch. Biochem. Biophys.* 484:114–116. http://dx.doi.org/10.1016/j.abb.2009.03.013

Beckman, J.S., T.W. Beckman, J. Chen, P.A. Marshall, and B.A. Freeman. 1990. Apparent hydroxyl radical production by peroxynitrite: implications for endothelial injury from nitric oxide and superoxide. *Proc. Natl. Acad. Sci. USA*. 87:1620–1624. http://dx.doi.org/10.1073/pnas.87.4.1620

Beckman, J.S., M. Carson, C.D. Smith, and W.H. Koppenol. 1993. ALS, SOD and peroxynitrite. *Nature*. 364:584. http://dx.doi.org/10.1038/364584a0

Beckman, J.S., J. Chen, H. Ischiropoulos, and J.P. Crow. 1994. Oxidative chemistry of peroxynitrite. *In* Oxygen Radicals in Biological Systems, Pt C. Academic Press.

Blum, D., S. Torch, N. Lambeng, M.F. Nissou, A.L. Benabid, R. Sadoul, and J.M. Verna. 2001. Molecular pathways involved in the neurotoxicity of 6-OHDA, dopamine and MPTP: contribution to the apoptotic theory in Parkinson's disease. *Prog. Neurobiol.* 65:135–172. http://dx.doi.org/10.1016/S0301-0082(01)00003-X

Cappai, R., S.L. Leck, D.J. Tew, N.A. Williamson, D.P. Smith, D. Galatis, R.A. Sharples, C.C. Curtain, F.E. Ali, R.A. Cherny, et al. 2005. Dopamine promotes alpha-synuclein aggregation into SDS-resistant soluble oligomers via a distinct folding pathway. *FASEB J.* 19:1377–1379.

Caudle, W.M., R.E. Colebrooke, P.C. Emson, and G.W. Miller. 2008. Altered vesicular dopamine storage in Parkinson's disease: a premature demise. *Trends Neurosci.* 31:303–308. http://dx.doi.org/10.1016/j.tins.2008.02.010

Cipriani, S., X.Q. Chen, and M.A. Schwarzschild. 2010. Urate: a novel biomarker of Parkinson's disease risk, diagnosis and prognosis. *Biomarkers Med.* 4:701–712. http://dx.doi.org/10.2217/bmm.10.94

Contestabile, A. 2008. Regulation of transcription factors by nitric oxide in neurons and in neural-derived tumor cells. *Prog. Neurobiol.* 84:317–328. http://dx.doi.org/10.1016/j.pneurobio.2008.01.002

Culvenor, J.G., C.A. McLean, S. Cutt, B.C. Campbell, F. Maher, P. Jäkälä, T. Hartmann, K. Beyreuther, C.L. Masters, and Q.X. Li. 1999. Non-Abeta component of Alzheimer's disease amyloid (NAC) revisited. NAC and α-synuclein are not associated with Abeta amyloid. *Am. J. Pathol.* 155:1173–1181. http://dx.doi.org/10.1016/S0002-9440(10)65220-0

Dauer, W., and S. Przedborski. 2003. Parkinson's disease: mechanisms and models.*Neuron*.39:889–909.http://dx.doi.org/10.1016/S0896-6273(03)00568-3

de Lau, L.M., P.J. Koudstaal, A. Hofman, and M.M. Breteler. 2005. Serum uric acid levels and the risk of Parkinson disease. *Ann. Neurol.* 58:797–800. http://dx.doi.org/10.1002/ana.20663

De Vera, M., M.M. Rahman, J. Rankin, J. Kopec, X. Gao, and H. Choi. 2008. Gout and the risk of Parkinson's disease: a cohort study. *Arthritis Rheum.* 59:1549–1554. http://dx.doi.org/10.1002/art.24193

Dehmer, T., J. Lindenau, S. Haid, J. Dichgans, and J.B. Schulz. 2000. Deficiency of inducible nitric oxide synthase protects against MPTP toxicity in vivo. *J. Neurochem.* 74:2213–2216. http://dx.doi.org/10.1046/j.1471-4159.2000.0742213.x

Dong, Z., B. Ferger, J. Feldon, and H. Büeler. 2002. Overexpression of Parkinson's disease-associated alpha-synucleinA53T by recombinant adeno-associated virus in mice does not increase the vulnerability of dopaminergic neurons to MPTP. *J. Neurobiol.* 53:1–10. http://dx.doi.org/10.1002/neu.10094

Donnelly, P.S., J.R. Liddell, S. Lim, B.M. Paterson, M.A. Cater, M.S. Savva, A.I. Mot, J.L. James, I.A. Trounce, A.R. White, and P.J. Crouch. 2012. An impaired mitochondrial electron transport chain increases retention of the hypoxia imaging agent diacetylbis(4-methylthiosemicarbazonato)copper II. *Proc. Natl. Acad. Sci. USA.* 109:47–52. http://dx.doi.org/10.1073/pnas.1116227108

Duda, J.E., B.I. Giasson, Q. Chen, T.L. Gur, H.I. Hurtig, M.B. Stern, S.M. Gollomp, H. Ischiropoulos, V.M. Lee, and J.Q. Trojanowski. 2000. Widespread nitration of pathological inclusions in neurodegenerative synucleinopathies. *Am. J. Pathol.* 157:1439–1445. http://dx.doi.org/10.1016/S0002-9440(10)64781-5

Ebadi, M., and S.K. Sharma. 2003. Peroxynitrite and mitochondrial dysfunction in the pathogenesis of Parkinson's disease. *Antioxid. Redox Signal.* 5:319–335. http://dx.doi.org/10.1089/152308603322110896

Ennaceur, A., and J. Delacour. 1988. A new one-trial test for neurobiological studies of memory in rats. 1: Behavioral data. *Behav. Brain Res.* 31:47–59. http://dx.doi.org/10.1016/0166-4328(88)90157-X

Feelisch, M., J. Ostrowski, and E. Noack. 1989. On the mechanism of NO release from sydnonimines. *J. Cardiovasc. Pharmacol.* 14:S13–S22.

Ferrante, R.J., P. Hantraye, E. Brouillet, and M.F. Beal. 1999. Increased nitrotyrosine immunoreactivity in substantia nigra neurons in MPTP treated baboons is blocked by inhibition of neuronal nitric oxide synthase. *Brain Res.* 823:177–182. http://dx.doi.org/10.1016/S0006-8993(99)01166-X

Finkelstein, D.I., D. Stanic, C.L. Parish, D. Tomas, K. Dickson, and M.K. Horne. 2000. Axonal sprouting following lesions of the rat substantia nigra. *Neuroscience.* 97:99–112. http://dx.doi.org/10.1016/S0306-4522(00)00009-9

Finkelstein, D.I., D. Stanic, C.L. Parish, J. Drago, and M.K. Horne. 2004. Quantified assessment of terminal density and innervation. *Curr. Protoc. Neurosci.* Chapter 1, Unit 113.

Fodero-Tavoletti, M.T., V.L. Villemagne, B.M. Paterson, A.R. White, Q.X. Li, J. Camakaris, G.J. O'Keefe, R. Cappai, K.J. Barnham, and P.S. Donnelly. 2010. Bis(thiosemicarbazonato) Cu-64 complexes for positron emission tomography imaging of Alzheimer's disease. *J. Alzheimers Dis.* 20:49–55.

Freichel, C., M. Neumann, T. Ballard, V. Müller, M. Woolley, L. Ozmen, E. Borroni, H.A. Kretzschmar, C. Haass, W. Spooren, and P.J. Kahle. 2007. Age-dependent cognitive decline and amygdala pathology in alpha-synuclein transgenic mice. *Neurobiol. Aging.* 28:1421–1435. http://dx.doi.org/10.1016/j.neurobiolaging.2006.06.013

Giasson, B.I., J.E. Duda, I.V. Murray, Q. Chen, J.M. Souza, H.I. Hurtig, H. Ischiropoulos, J.Q. Trojanowski, and V.M. Lee. 2000. Oxidative damage linked to neurodegeneration by selective α-synuclein nitration in synucleinopathylesions.*Science*.290:985–989.http://dx.doi.org/10.1126/science.290.5493.985

Giasson, B.I., J.E. Duda, S.M. Quinn, B. Zhang, J.Q. Trojanowski, and V.M. Lee. 2002. Neuronal α-synucleinopathy with severe movement disorder in mice expressing A53T human α-synuclein. *Neuron.* 34:521–533. http://dx.doi.org/10.1016/S0896-6273(02)00682-7

Good, P.F., A. Hsu, P. Werner, D.P. Perl, and C.W. Olanow. 1998. Protein nitration in Parkinson's disease. *J. Neuropathol. Exp. Neurol.* 57:338–342. http://dx.doi.org/10.1097/00005072-199804000-00006

Gundersen, H.J., P. Bagger, T.F. Bendtsen, S.M. Evans, L. Korbo, N. Marcussen, A. Møller, K. Nielsen, J.R. Nyengaard, B. Pakkenberg, et al. 1988. The new stereological tools: disector, fractionator, nucleator and point sampled intercepts and their use in pathological research and diagnosis. *APMIS.* 96:857–881. http://dx.doi.org/10.1111/j.1699-0463.1988.tb00954.x

Gupta, S.P., S. Patel, S. Yadav, A.K. Singh, S. Singh, and M.P. Singh. 2010. Involvement of nitric oxide in maneb- and paraquat-induced Parkinson's disease phenotype in mouse: is there any link with lipid peroxidation? *Neurochem. Res.* 35:1206–1213. http://dx.doi.org/10.1007/s11064-010-0176-5

Hantraye, P., E. Brouillet, R. Ferrante, S. Palfi, R. Dolan, R.T. Matthews, and M.F. Beal. 1996a. Inhibition of neuronal nitric oxide synthase prevents MPTP-induced parkinsonism in baboons. *Nat. Med.* 2:1017–1021. http://dx.doi.org/10.1038/nm0996-1017

Hantraye, P., E. Brouillet, R. Ferrante, S. Palfi, R. Dolan, R.T. Matthews, and M.F. Beal. 1996b. Inhibition of neuronal nitric oxide synthase prevents MPTP-induced parkinsonism in baboons. *Nat. Med.* 2:1017–1021. http://dx.doi.org/10.1038/nm0996-1017

Hassler, R. 1938. Pathologie der Paralysis agitans und des postenzephailitischen Parkinsonismus. *J. Psychol. Neurol.* 48:387–476.

Hefti, F.F., H.F. Kung, M.R. Kilbourn, A.P. Carpenter, C.M. Clark, and D.M. Skovronsky. 2010. ^{18}F-AV-133: A Selective VMAT2-binding Radiopharmaceutical for PET Imaging of Dopaminergic Neurons. *PET Clin.* 5:75–82. http://dx.doi.org/10.1016/j.cpet.2010.02.001

Henze, C., C. Earl, J. Sautter, N. Schmidt, C. Themann, A. Hartmann, and W.H. Oertel. 2005. Reactive oxidative and nitrogen species in the nigrostriatal system following striatal 6-hydroxydopamine lesion in rats. *Brain Res.* 1052:97–104. http://dx.doi.org/10.1016/j.brainres.2005.06.020

Hooper, D.C., S. Spitsin, R.B. Kean, J.M. Champion, G.M. Dickson, I. Chaudhry, and H. Koprowski. 1998. Uric acid, a natural scavenger of peroxynitrite, in experimental allergic encephalomyelitis and multiple sclerosis. *Proc. Natl. Acad. Sci. USA.* 95:675–680. http://dx.doi.org/10.1073/pnas.95.2.675

Ikawa, M., H. Okazawa, T. Kudo, M. Kuriyama, Y. Fujibayashi, and M. Yoneda. 2011. Evaluation of striatal oxidative stress in patients with Parkinson's disease using [62Cu]ATSM PET. *Nucl. Med. Biol.* 38:945–951. http://dx.doi.org/10.1016/j.nucmedbio.2011.02.016

Jackson-Lewis, V., and S. Przedborski. 2007. Protocol for the MPTP mouse model of Parkinson's disease. *Nat. Protocol.* 2:141–151.

Kanner, B.I., and S. Schuldiner. 1987. Mechanism of transport and storage of neurotransmitters. *CRC Crit. Rev. Biochem.* 22:1–38. http://dx.doi.org/10.3109/10409238709082546

Kastner, A., E.C. Hirsch, Y. Agid, and F. Javoy-Agid. 1993. Tyrosine hydroxylase protein and messenger RNA in the dopaminergic nigral neurons of patients with Parkinson's disease. *Brain Res.* 606:341–345. http://dx.doi.org/10.1016/0006-8993(93)91005-D

Kazantsev, A.G., and A.M. Kolchinsky. 2008. Central role of alpha-synuclein oligomers in neurodegeneration in Parkinson disease. *Arch. Neurol.* 65:1577–1581. http://dx.doi.org/10.1001/archneur.65.12.1577

Langston, J.W., P. Ballard, J.W. Tetrud, and I. Irwin. 1983. Chronic Parkinsonism in humans due to a product of meperidine-analog synthesis. *Science.* 219:979–980. http://dx.doi.org/10.1126/science.6823561

Lee, M.K., W. Stirling, Y. Xu, X. Xu, D. Qui, A.S. Mandir, T.M. Dawson, N.G. Copeland, N.A. Jenkins, and D.L. Price. 2002. Human alpha-synuclein-harboring familial Parkinson's disease-linked Ala-53 —> Thr mutation causes neurodegenerative disease with alpha-synuclein aggregation in transgenic mice. *Proc. Natl. Acad. Sci. USA.* 99:8968–8973. http://dx.doi.org/10.1073/pnas.132197599

Lee, J., W.M. Zhu, D. Stanic, D.I. Finkelstein, M.H. Horne, J. Henderson, A.J. Lawrence, L. O'Connor, D. Tomas, J. Drago, and M.K. Horne. 2008.

Sprouting of dopamine terminals and altered dopamine release and uptake in Parkinsonian dyskinaesia. *Brain*. 131:1574–1587. http://dx.doi.org/10.1093/brain/awn085

Lee, J.R., J.K. Kim, S.J. Lee, and K.P. Kim. 2009. Role of protein tyrosine nitration in neurodegenerative diseases and atherosclerosis. *Arch. Pharm. Res.* 32:1109–1118. http://dx.doi.org/10.1007/s12272-009-1802-0

Leong, S.L., C.L. Pham, D. Galatis, M.T. Fodero-Tavoletti, K. Perez, A.F. Hill, C.L. Masters, F.E. Ali, K.J. Barnham, and R. Cappai. 2009. Formation of dopamine-mediated alpha-synuclein-soluble oligomers requires methionine oxidation. *Free Radic. Biol. Med.* 46:1328–1337. http://dx.doi.org/10.1016/j.freeradbiomed.2009.02.009

Lewis, J., R. Laforest, T. Buettner, S. Song, Y. Fujibayashi, J. Connett, and M. Welch. 2001. Copper-64-diacetyl-bis(N4-methylthiosemicarbazone): An agent for radiotherapy. *Proc. Natl. Acad. Sci. USA*. 98:1206–1211. http://dx.doi.org/10.1073/pnas.98.3.1206

LeWitt, P.A. 2004. Clinical trials of neuroprotection for Parkinson's disease. *Neurology*. **63**:S23–S31.

Lewy, F.H. 1912. Paralysis Agitans. I. Pathologische Antomie. *In:* Lewandowsky, M. (ed.) *Handbuch der Neurologie*. Berlin: Julius Springer.

Lim, Y., V.M. Kehm, E.B. Lee, J.H. Soper, C. Li, J.Q. Trojanowski, and V.M.Y. Lee. 2011. α-Syn suppression reverses synaptic and memory defects in a mouse model of dementia with Lewy bodies. *J. Neurosci.* 31:10076–10087. http://dx.doi.org/10.1523/JNEUROSCI.0618-11.2011

Maries, E., B. Dass, T.J. Collier, J.H. Kordower, and K. Steece-Collier. 2003. The role of α-synuclein in Parkinson's disease: insights from animal models. *Nat. Rev. Neurosci.* 4:727–738. http://dx.doi.org/10.1038/nrn1199

Martin, L.J., Y. Pan, A.C. Price, W. Sterling, N.G. Copeland, N.A. Jenkins, D.L. Price, and M.K. Lee. 2006. Parkinson's disease alpha-synuclein transgenic mice develop neuronal mitochondrial degeneration and cell death. *J. Neurosci.* 26:41–50. http://dx.doi.org/10.1523/JNEUROSCI.4308-05.2006

Matsuura, K., H. Kabuto, H. Makino, and N. Ogawa. 1997. Pole test is a useful method for evaluating the mouse movement disorder caused by striatal dopamine depletion. *J. Neurosci. Methods*. 73:45–48. http://dx.doi.org/10.1016/S0165-0270(96)02211-X

Meredith, G.E., and U.J. Kang. 2006. Behavioral models of Parkinson's disease in rodents: a new look at an old problem. *Mov. Disord.* 21:1595–1606. http://dx.doi.org/10.1002/mds.21010

Meredith, G.E., S. Totterdell, E. Petroske, K. Santa Cruz, R.C. Callison Jr., and Y.S. Lau. 2002. Lysosomal malfunction accompanies alpha-synuclein aggregation in a progressive mouse model of Parkinson's disease. *Brain Res.* 956:156–165. http://dx.doi.org/10.1016/S0006-8993(02)03514-X

Meredith, G.E., P.K. Sonsalla, and M.F. Chesselet. 2008. Animal models of Parkinson's disease progression. *Acta Neuropathol.* 115:385–398. http://dx.doi.org/10.1007/s00401-008-0350-x

Nebot, C., M. Moutet, P. Huet, J.Z. Xu, J.C. Yadan, and J. Chaudiere. 1993. Spectrophotometric assay of superoxide dismutase activity based on the activated autoxidation of a tetracyclic catechol. *Anal. Biochem.* 214:442–451. http://dx.doi.org/10.1006/abio.1993.1521

Neystat, M., T. Lynch, S. Przedborski, N. Kholodilov, M. Rzhetskaya, and R.E. Burke. 1999. Alpha-synuclein expression in substantia nigra and cortex in Parkinson's disease. *Mov. Disord.* 14:417–422.

Obeso, J.A., M.C. Rodriguez-Oroz, C.G. Goetz, C. Marin, J.H. Kordower, M. Rodriguez, E.C. Hirsch, M. Farrer, A.H. Schapira, and G. Halliday. 2010. Missing pieces in the Parkinson's disease puzzle. *Nat. Med.* 16:653–661. http://dx.doi.org/10.1038/nm.2165

Oehlberg, K., F.K. Barg, G.K. Brown, D. Taraborelli, M.B. Stern, and D. Weintraub. 2008. Attitudes regarding the etiology and treatment of depression in Parkinson's disease: a qualitative study. *J. Geriatr. Psychiatry Neurol.* 21:123–132. http://dx.doi.org/10.1177/0891988708316862

Ogawa, N., Y. Hirose, S. Ohara, T. Ono, and Y. Watanabe. 1985. A simple quantitative bradykinesia test in MPTP-treated mice. *Res. Commun. Chem. Pathol. Pharmacol.* 50:435–441.

Ogawa, N., K. Mizukawa, Y. Hirose, S. Kajita, S. Ohara, and Y. Watanabe. 1987. MPTP-induced parkinsonian model in mice: biochemistry, pharmacology and behavior. *Eur. Neurol.* 26:16–23. http://dx.doi.org/10.1159/000116351

Pakkenberg, B., A. Møller, H.J. Gundersen, A. Mouritzen Dam, and H. Pakkenberg. 1991.The absolute number of nerve cells in substantia nigra in normal subjects and in patients with Parkinson's disease estimated with an unbiased stereological method. *J. Neurol. Neurosurg. Psychiatry*. 54:30–33. http://dx.doi.org/10.1136/jnnp.54.1.30

Parish, C.L., D.I. Finkelstein, J. Drago, E. Borrelli, and M.K. Horne. 2001. The role of dopamine receptors in regulating the size of axonal arbors. *J. Neurosci.* 21:5147–5157.

Parkinson, J. 2002. An essay on the shaking palsy. 1817. *J. Neuropsychiatry Clin. Neurosci.* 14:223–236. http://dx.doi.org/10.1176/appi.neuropsych.14.2.223

Parkinson Study Group. 2004. The safety and tolerability of a mixed lineage kinase inhibitor (CEP-1347) in PD. *Neurology*. 62:330–332.

Parkinson Study Group PRECEPT Investigators. 2007. Mixed lineage kinase inhibitor CEP-1347 fails to delay disability in early Parkinson disease. *Neurology*. 69:1480–1490. http://dx.doi.org/10.1212/01.wnl.0000277648.63931.c0

Paxinou, E., Q. Chen, M. Weisse, B.I. Giasson, E.H. Norris, S.M. Rueter, J.Q. Trojanowski, V.M. Lee, and H. Ischiropoulos. 2001. Induction of α-synuclein aggregation by intracellular nitrative insult. *J. Neurosci.* 21: 8053–8061.

Pham, C.L., S.L. Leong, F.E. Ali, V.B. Kenche, A.F. Hill, S.L. Gras, K.J. Barnham, and R. Cappai. 2009. Dopamine and the dopamine oxidation product 5,6-dihydroxylindole promote distinct on-pathway and off-pathway aggregation of alpha-synuclein in a pH-dependent manner. *J. Mol. Biol.* 387:771–785. http://dx.doi.org/10.1016/j.jmb.2009.02.007

Pierucci, M., S. Galati, M. Valentino, V. Di Matteo, A. Benigno, R. Muscat, A. Pitruzzella, and G. Di Giovanni. 2011. Nitric Oxide Modulation Of The Basal Ganglia Circuitry: Therapeutic Implication For Parkinson's Disease And Other Motor Disorders. *CNS Neurol. Disord. Drug Targets*. (Epub ahead of print).

Presgraves, S.P., T. Ahmed, S. Borwege, and J.N. Joyce. 2004. Terminally differentiated SH-SY5Y cells provide a model system for studying neuroprotective effects of dopamine agonists. *Neurotox. Res.* 5:579–598. http://dx.doi.org/10.1007/BF03033178

Przedborski, S., V. Jackson-Lewis, R. Yokoyama, T. Shibata, V.L. Dawson, and T.M. Dawson. 1996. Role of neuronal nitric oxide in 1-methyl-4-phenyl-1,2,3,6-tetrahydropyridine (MPTP)-induced dopaminergic neurotoxicity. *Proc. Natl. Acad. Sci. USA*. 93:4565–4571. http://dx.doi.org/10.1073/pnas.93.10.4565

Przedborski, S., Q.P. Chen, M. Vila, B.I. Giasson, R. Djaldatti, S. Vukosavic, J.M. Souza, V. Jackson-Lewis, V.M.Y. Lee, and H. Ischiropoulos. 2001. Oxidative post-translational modifications of alpha-synuclein in the 1-methyl-4-phenyl-1,2,3,6-tetrahydropyridine (MPTP) mouse model of Parkinson's disease. *J. Neurochem.* 76:637–640. http://dx.doi.org/10.1046/j.1471-4159.2001.00174.x

Przedborski, S., V. Jackson-Lewis, M. Vila, D.C. Wu, P. Teismann, K. Tieu, D.K. Choi, and O. Cohen. 2003. Free radical and nitric oxide toxicity in Parkinson's disease. *Adv. Neurol.* 91:83–94.

Reynolds, M.R., R.W. Berry, and L.I. Binder. 2007. Nitration in neurodegeneration: deciphering the "Hows" "nYs". *Biochemistry*. 46:7325–7336. http://dx.doi.org/10.1021/bi700430y

Saporito, M.S., E.M. Brown, M.S. Miller, and S. Carswell. 1999. CEP-1347/KT-7515, an inhibitor of c-jun N-terminal kinase activation, attenuates the 1-methyl-4-phenyl tetrahydropyridine-mediated loss of nigrostriatal dopaminergic neurons In vivo. *J. Pharmacol. Exp. Ther.* 288:421–427.

Schapira, A.H.V. 2008. Mitochondria in the aetiology and pathogenesis of Parkinson's disease. *Lancet Neurol.* 7:97–109. http://dx.doi.org/10.1016/S1474-4422(07)70327-7

Schlüter, O.M., F. Fornai, M.G. Alessandrí, S. Takamori, M. Geppert, R. Jahn, and T.C. Südhof. 2003. Role of α-synuclein in 1-methyl-4-phenyl-1,2,3,6-tetrahydropyridine-induced parkinsonism in mice. *Neuroscience*. 118:985–1002. http://dx.doi.org/10.1016/S0306-4522(03)00036-8

Schulz, J.B. 2008. Update on the pathogenesis of Parkinson's disease. *J. Neurol.* 255:3–7. http://dx.doi.org/10.1007/s00415-008-5011-4

Schulz, J.B., R.T. Matthews, M.M. Muqit, S.E. Browne, and M.F. Beal. 1995. Inhibition of neuronal nitric oxide synthase by 7-nitroindazole protects against MPTP-induced neurotoxicity in mice. *J. Neurochem.* 64:936–939. http://dx.doi.org/10.1046/j.1471-4159.1995.64020936.x

Sedelis, M., R.K. Schwarting, and J.P. Huston. 2001. Behavioral phenotyping of the MPTP mouse model of Parkinson's disease. *Behav. Brain Res.* 125:109–125. http://dx.doi.org/10.1016/S0166-4328(01)00309-6

Soon, C.P., P.S. Donnelly, B.J. Turner, L.W. Hung, P.J. Crouch, N.A. Sherratt, J.L. Tan, N.K. Lim, L. Lam, L. Bica, et al. 2011. Diacetylbis(N(4)-methylthiosemicarbazonato) copper(II) (CuII(atsm)) protects against peroxynitrite-induced nitrosative damage and prolongs survival in amyotrophic lateral sclerosis mouse model. *J. Biol. Chem.* 286:44035–44044. http://dx.doi.org/10.1074/jbc.M111.274407

Souza, J.M., B.I. Giasson, Q. Chen, V.M. Lee, and H. Ischiropoulos. 2000. Dityrosine cross-linking promotes formation of stable α -synuclein polymers. Implication of nitrative and oxidative stress in the pathogenesis of neurodegenerative synucleinopathies. *J. Biol. Chem.* 275:18344–18349. http://dx.doi.org/10.1074/jbc.M000206200

Stanic, D., D.I. Finkelstein, D.W. Bourke, J. Drago, and M.K. Horne. 2003a. Timecourse of striatal re-innervation following lesions of dopaminergic SNpc neurons of the rat. *Eur. J. Neurosci.* 18:1175–1188. http://dx.doi.org/10.1046/j.1460-9568.2003.02800.x

Stanic, D., C.L. Parish, W.M. Zhu, E.V. Krstew, A.J. Lawrence, J. Drago, D.I. Finkelstein, and M.K. Horne. 2003b. Changes in function and ultrastructure of striatal dopaminergic terminals that regenerate following partial lesions of the SNpc. *J. Neurochem.* 86:329–343. http://dx.doi.org/10.1046/j.1471-4159.2003.01843.x

Stowe, R.L., N.J. Ives, C. Clarke, J. van Hilten, J. Ferreira, R.J. Hawker, L. Shah, K. Wheatley, and R. Gray. 2008. Dopamine agonist therapy in early Parkinson's disease. *Cochrane Database Syst. Rev.* (2):CD006564.

Szabó, C., H. Ischiropoulos, and R. Radi. 2007. Peroxynitrite: biochemistry, pathophysiology and development of therapeutics. *Nat. Rev. Drug Discov.* 6:662–680. http://dx.doi.org/10.1038/nrd2222

Terzioglu, M., and D. Galter. 2008. Parkinson's disease: genetic versus toxin-induced rodent models. *FEBS J.* 275:1384–1391. http://dx.doi.org/10.1111/j.1742-4658.2008.06302.x

Thomas, B., and M.F. Beal. 2007. Parkinson's disease. *Hum. Mol. Genet.* 16:R183–R194. http://dx.doi.org/10.1093/hmg/ddm159

Trackey, J.L., T.F. Uliasz, and S.J. Hewett. 2001. SIN-1-induced cytotoxicity in mixed cortical cell culture: peroxynitrite-dependent and -independent induction of excitotoxic cell death. *J. Neurochem.* 79:445–455. http://dx.doi.org/10.1046/j.1471-4159.2001.00584.x

Trost, M., S. Su, P. Su, R.F. Yen, H.M. Tseng, A. Barnes, Y. Ma, and D. Eidelberg. 2006. Network modulation by the subthalamic nucleus in the treatment of Parkinson's disease. *Neuroimage.* 31:301–307. http://dx.doi.org/10.1016/j.neuroimage.2005.12.024

Wang, J.L., S. Oya, A.K. Parhi, B.P. Lieberman, K. Ploessl, C. Hou, and H.F. Kung. 2010. In vivo studies of the SERT-selective [18F]FPBM and VMAT2-selective [18F]AV-133 radiotracers in a rat model of Parkinson's disease. *Nucl. Med. Biol.* 37:479–486. http://dx.doi.org/10.1016/j.nucmedbio.2010.01.006

Watabe, M., and T. Nakaki. 2008. Mitochondrial complex I inhibitor rotenone inhibits and redistributes vesicular monoamine transporter 2 via nitration in human dopaminergic SH-SY5Y cells. *Mol. Pharmacol.* 74:933–940. http://dx.doi.org/10.1124/mol.108.048546

Weintraub, D., C.L. Comella, and S. Horn. 2008. Parkinson's disease—Part 3: Neuropsychiatric symptoms. *Am. J. Manag. Care.* 14:S59–S69.

West, M.J., and H.J. Gundersen. 1990. Unbiased stereological estimation of the number of neurons in the human hippocampus. *J. Comp. Neurol.* 296:1–22. http://dx.doi.org/10.1002/cne.902960102

Wills, J., J. Credle, T. Haggerty, J.-H. Lee, A.W. Oaks, and A. Sidhu. 2011. Tauopathic changes in the striatum of A53T α-synuclein mutant mouse model of Parkinson's disease. *PLoS ONE.* 6:e17953. http://dx.doi.org/10.1371/journal.pone.0017953

Yu, W.H., Y. Matsuoka, I. Sziráki, A. Hashim, J. Lafrancois, H. Sershen, and K.E. Duff. 2008. Increased dopaminergic neuron sensitivity to 1-methyl-4-phenyl-1,2,3,6-tetrahydropyridine (MPTP) in transgenic mice expressing mutant A53T alpha-synuclein. *Neurochem. Res.* 33:902–911. http://dx.doi.org/10.1007/s11064-007-9533-4

Yu, Z.W., X.H. Xu, Z.H. Xiang, J.F. Zhou, Z.H. Zhang, C. Hu, and C. He. 2010. Nitrated alpha-synuclein induces the loss of dopaminergic neurons in the substantia nigra of rats. *PLoS ONE.* 5:e9956. http://dx.doi.org/10.1371/journal.pone.0009956

Zhang, M.Y., N. Kagan, M.L. Sung, M.M. Zaleska, and M. Monaghan. 2008. Sensitive and selective liquid chromatography/tandem mass spectrometry methods for quantitative analysis of 1-methyl-4-phenyl pyridinium (MPP+) in mouse striatal tissue. *J. Chromatogr. B Analyt. Technol. Biomed. Life Sci.* 874:51–56. http://dx.doi.org/10.1016/j.jchromb.2008.08.030